

Robust Integrated Data and Energy Transfer Aided by Intelligent Reflecting Surfaces: Successive Target Migration Optimization Towards Energy Sustainability

Qingdong Yue, Jie Hu, *Senior Member, IEEE*, Kun Yang, *Fellow, IEEE*, Kai-Kit Wong, *Fellow, IEEE*

Abstract—Intelligent reflecting surfaces (IRSs) can actively adjust the wireless environment. However, accurate channel estimation on IRS-aided communication systems is difficult to obtain. Therefore, we study a robust beamforming design for an IRS-aided integrated data and energy transfer (IDET) with imperfect channel state information (CSI). Against the uncertain channel estimation error, we robustly design the transmit beamformers of the transmitter and the passive reflecting beamformer of the IRS to minimize the transmit power by satisfying both the wireless data transfer (WDT) and wireless energy transfer (WET) requirements for realising energy-sustainability in 6G. A successive target migration optimization (STMO) algorithm is proposed to obtain a robust design. The transmit covariance matrices are optimized by relaxing rank-one constraints, when a passive reflecting beamformer is given. Then, the target to minimize the transmit power is migrated to maximize the QoS requirements of energy users due to the fixed transmit power. A local optimal reflecting beamformer is obtained for improving the attainable WET performance, when the transmit covariance matrices are given. Finally, we prove that the rank-one transmit beamformers can always be found, which have the same WET and WDT performance as the transmit covariance matrices. The numerical results demonstrate the advantage of our design.

Index Terms—Integrated data and energy transfer (IDET), intelligent reflecting surface (IRS), non-linear energy harvester, imperfect channel state information (CSI), robust design, successive target migration optimization (STMO), energy sustainability

Qingdong Yue and Jie Hu are with the School of Information and Communication Engineering, University of Electronic Science and Technology of China, Chengdu, 611731, China, email: qdyue1588@163.com and hujie@uestc.edu.cn

Kun Yang is with the School of Information and Communication Engineering, University of Electronic Science and Technology of China, Chengdu 611731, China and also with the School of Computer Science and Electronic Engineering, University of Essex, Colchester, CO4 3SQ, U.K. email: kyang@ieee.org.

Kai-Kit Wong is with the Department of Electronic and Electrical Engineering, University College London, United Kingdom, WC1E 6BT, email: kai-kit.wong@ucl.ac.uk.

The authors would like to thank the financial support of National Natural Science Foundation of China, No. 61971102, that of Sichuan Science and Technology Program, No. 2022YFH0022, that of Natural Science Foundation of China, No. 62132004, that of MOST Major Research and Development Project, No. 2021YFB2900204, that of Sichuan Major R&D Project, No. 22QYCX0168, that of the Municipal Government of Quzhou, No.: 2022D031 and that of EU H2020 Project COSAFE, GA-824019.

I. INTRODUCTION

A. Background and Motivation

The number of Internet of Everything (IoE) devices is expected to increase from about 7 billion in 2018 to 22 billion by 2025, laying the foundation of the future smart home, smart industry and smart city [1], [2]. However, the IoE devices are suffering from the problem of energy supplement [3], [4]. Therefore, radio-frequency (RF) signals are relied upon for providing integrated data and energy transfer (IDET) services towards them [5], [6]. In order to achieve energy-sustainability in future 6G, we should substantially reduce the energy consumption by satisfying both the data and energy requirements of IoE devices [7].

In order to overcome the adverse effect induced by the large path-loss, multiple antennas at transmitters are implemented for the sake of substantially improving the IDET performance [7], [8]. Furthermore, intelligent reflecting surface (IRS) with massive low-cost passive reflecting elements was regarded as a promising technology to improve the performance of next generation wireless communication [9]. Moreover, IRS was also implemented to improve the IDET performance towards IoE devices, by providing enormous spatial gains [10].

However, the channel estimations of the IRS cascaded channels is not very accurate. This is because the IRS has no RF chains and the number of reflectors in the IRS is far larger than the number of antennas in the transmitter, which results insufficient degree of freedom for channel estimation. Therefore, the robust beamforming design is required in an IRS aided IDET system.

B. Related Works

There are many beamforming design in MIMO and IRS system. For example, Park *et al.* [11] studied the multiple-input-multiple-output (MIMO) full-duplex wireless powered communication network (WPCN). They optimized the user selection, antenna switching and beamforming to maximize the average sum-rate, while satisfying energy requirements. Ma *et al.* [12] designed the energy beamformer and information beamformer in the massive MIMO system to maximize the sum-rate. Zhu *et al.* [13] considered the secrecy IDET mmWave system. They jointly designed the digital beamformer, artificial noise matrix and power splitting ratio

to maximize the secrecy rate, while satisfying energy requirements. Hu *et al.* [14] designed the transmit beamformer and receive combining for the sake of maximizing the fair-throughput in the MIMO WPCN system subject to the energy requirements. However, efficient design to reduce the huge energy consumption of delivering IDET services has not been considered yet. Specifically, Wu *et al.* [15] studied an IRS-assisted IDET system, where the transmit precoder and the passive reflecting beamformer are jointly optimized for minimizing the transmit power, subject to the quality-of-service (QoS) constraints at all users. Zou *et al.* [16] investigated a wireless powered IRS for communications. The IRS could work in both energy harvesting mode and signal reflecting mode. The maximum achievable rate was obtained by optimizing the transmit beamformer, the passive reflecting beamformer and the IRS's time allocation between these two modes. Pan *et al.* [17] studied an IRS-aided IDET system. To maximize the weighted sum-rate, the transmit precoders and passive reflecting beamformer were jointly optimized by guaranteeing the energy harvesting requirements of energy receivers. IRS is also applied for sensing. Shao *et al.* [18] proposed a new self-sensing IRS architecture where it's capable of both transmitting and reflecting signals. Hu *et al.* [19] proposed an IRS aided integrated sensing and communication (ISAC), where the transmission protocol, location sensing and beamforming optimization. Yu *et al.* [20] investigated the IRS aided multi-user ISAC system, where IRS assists the data transmission and conducts the user localization.

All the above-mentioned works assumed that the CSI was perfect for both transmitters and receivers. However, accurate channel estimations on IRS related channels were challenging in practice [21], [22]. Wang *et al.* [21] proposed a three-phase framework of a pilot-based channel estimation for IRS-assisted uplink multiuser communications. Direct user to base station (BS) channels and a single user-IRS-BS reflected channel were firstly estimated, respectively, while the other user-IRS-BS reflected channels were estimated. Arajo *et al.* [23] invoked a tensor modelling approach by using pilots to estimate the channel of an IRS aided MIMO communication system. Zhou *et al.* [22] considered that a BS-IRS-user link was decomposed into multiple sub-channels, each of which corresponds to a single IRS element. Then these sub-channels were estimated one-by-one.

However, since there are too many passive reflecting elements in an IRS, the channel estimations were not as accurate as traditional MIMO system. Therefore, a robust design for an IRS-aided communication system is essential, which represents a design with imperfect channel state information (CSI). Zhou *et al.* [24] considered a robust beamforming scheme for an IRS-aided multi-user (UE) MIMO system under an assumption of imperfect CSI. They aimed for minimizing the transmit power, while satisfying the achievable rate requirements of all users for all possible realizations of channel estimation errors. Niu *et al.* [25] investigated a robust design of an IRS aided secure IDET wireless communication system. They designed a transmit beamformer and an artificial-noise covariance matrix of the transmitter as well as the passive reflecting beamformer of the IRS to maximize the minimum

achievable rate, subject to the outage probability constraints with statistical cascaded CSI errors. Yu *et al.* [26] investigated an IRS aided IDET system by considering the outage-constrained robust design under imperfect CSI.

In a nutshell, the existing works on the design of IRS aided IDET system has the following drawbacks:

- Some works [10], [27]–[29] impractically assumed perfect CSI, since accurate CSI of the transmitter-IRS-UE link is difficult to be obtained. Some works [24], [30] in robust design of IRS aided WDT only considered a transmitter-IRS-UE link, while ignoring the direct transmitter-UE link. By taking these two links into account, both WDT and wireless energy transfer (WET) performance can be substantially improved.
- Some work [25] maximized the achievable rate in a robust IRS aided IDET system. However, a robust design of IRS aided IDET to minimize the transmit power is also important to achieve energy-sustainability in future 6G.
- In the IRS aided MIMO-IDET robust design, the transmit beamformers and passive beamformer are optimized alternately. Some works [30]–[32] only design the transmit covariance matrices of the transmit beamformers by relaxing the rank-one constraints with the classic semi-definite programming (SDP). However, only the rank-one transmit beamformer can be practically implemented. Some works [30], [33] recovered the rank-one beamformer in robust and secure communication system. However, how to recover the transmit beamformer from the covariance matrices without performance loss in an IDET system is still an open problem.
- In the robust passive beamformer design of the IRS, some work [31] optimized the passive beamformer to simultaneously improve the WDT and WET performance in the IDET system, while [32] solved the feasibility check problem associated with passive beamformer when the transmit beamformer is given in the IDET system. However, the convergence in both [31] and [32] cannot be guaranteed. Therefore, we need to carefully design the passive beamformer in a robust IRS aided IDET system.

C. Novel Contributions

In order to overcome the above-mentioned drawbacks, our novel contributions are summarized as below:

- We investigate an IRS aided energy sustainable network for achieving the following two goals: 1) Reduce the transmit power of the transmitter; 2) Provide IDET services to both data users (DUs) and energy users (EUs). Active transmit beamformers of the transmitter and passive reflecting beamformers of the IRS are jointly designed for the sake of minimizing the transmit power with imperfect CSI, while the QoS requirements of both DUs and EUs are satisfied.
- A successive target migration optimization (STMO) algorithm is proposed to minimize the transmit power, whose convergence is proved. Given a fixed passive reflecting beamformer, by relaxing the rank-one constraints, a sub-problem of optimizing the transmit covariance matrices

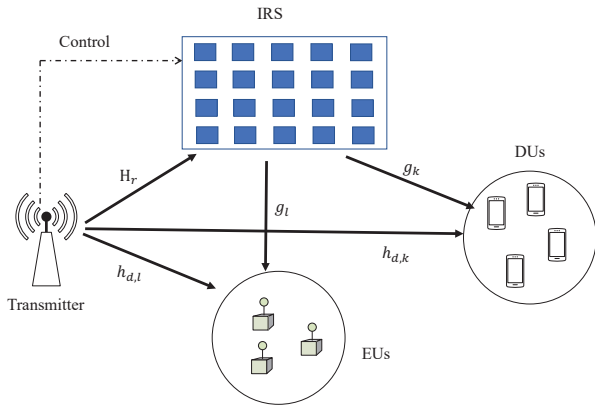


Fig. 1. IRS added MIMO system.

to minimize the transmit power is converted to a convex optimization problem. Given a fixed transmit covariance matrices, the target to minimize the transmit power is migrated to maximize the QoS requirements of EUs. A local optimal reflecting beamformer is obtained for improving the attainable WET performance, while satisfying the WDT requirements. We then prove that the transmit power reduces in the next iteration, if the optimum WET performance is higher than the constraints.

- We prove that the rank-one transmit beamformers can be always found, which has the same WET and WDT performance as the transmit covariance matrices.
- Numerical results verify the performance advantage of our robust design. We demonstrate that the transmit power increases with higher WDT or WET requirements. The transmit power decreases with more reflector in the IRS due to the increased spatial gain. Furthermore, the transmit power increases with higher estimation errors.

The rest of the paper is organized as follows: Our system model is introduced in Section II, while both the problem formulation and the optimal joint design are obtained in Section III. After presenting pivotal numerical results in Section IV, our paper is concluded in Section V.

Notation: $(\cdot)^H$ denotes transpose-conjugate operations. $|a|$ and $\|\mathbf{a}\|$ are the magnitude and norm of a scalar a and vector \mathbf{a} . $\|\mathbf{A}\|_F$ denotes the Frobenius norm of matrix \mathbf{A} . $\mathbf{A}(i, j)$ represents the element at the i -th row and the j -th column in \mathbf{A} . $\text{vec}(\mathbf{A})$ is the vectorization of matrix \mathbf{A} . $\text{diag}(\mathbf{a})$ is the diagonal matrix generated by the vector \mathbf{a} . DU_k and EU_l represent the k -th DU and the l -th EU. \otimes is the Kronecher inner product. $\text{var}(a)$ is the variance of random variable a .

II. SYSTEM MODEL

An IRS aided MISO-IDET system consists of a single transmitter equipped with $N_t > 1$ antennas, an IRS equipped with $M > 1$ passive reflectors, K data users (DUs) and L energy users (EUs) both equipped with a single antenna. The EUs are usually low-power wireless sensors, which needs to be remotely recharged. The wireless channel from the transmitter to the IRS, that from the IRS to the k -th DU

(DU_k) or the l -th EU (EU_l) and that from the transmitter to DU_k or EU_l are denoted as $\mathbf{H}_r \in \mathbb{C}^{M \times N_t}$, $\mathbf{g}_k \in \mathbb{C}^{M \times 1}$ or $\mathbf{g}_l \in \mathbb{C}^{M \times 1}$, and $\mathbf{h}_{d,k} \in \mathbb{C}^{N_t \times 1}$ or $\mathbf{h}_{d,l} \in \mathbb{C}^{N_t \times 1}$, respectively, as illustrated in Fig.1.

The transmitter broadcasts the Gaussian data symbols $\mathbf{s} = [s_1, s_2, \dots, s_K]$ to all users, where s_i is a 1×1 complex scalar satisfying a complex Gaussian distribution, i.e., $s_i \sim \mathcal{CN}(0, 1)$. The transmitter also broadcasts N_t energy flows $\mathbf{s}_E \in \mathbb{C}^{N_t \times 1}$ to recharge all EUs, where $s_E(j) \sim \mathcal{CN}(0, 1)$ for $\forall j$. Denote that the phase-shifter of the m -th passive reflector of the IRS by a complex number ϕ_m satisfying $|\phi_m| = 1$. Therefore, the passive reflector simply multiplies the incident multi-path signals by ϕ_m and it then reflects the adjusted signal to the DUs and EUs. The k -th DU and l -th EU receive the RF signal directly transmitted by the transmitter and that reflected by the IRS, which are then expressed as

$$y_k = (\mathbf{h}_{d,k}^H + \mathbf{g}_k^H \Phi \mathbf{H}_r) \left(\sum_{i=1}^K \mathbf{f}_i s_i + \mathbf{F}_E \mathbf{s}_E \right) + n_k, \quad k = 1, \dots, K, \quad (1)$$

$$y_l = (\mathbf{h}_{d,l}^H + \mathbf{g}_l^H \Phi \mathbf{H}_r) \left(\sum_{i=1}^K \mathbf{f}_i s_i + \mathbf{F}_E \mathbf{s}_E \right) + n_l, \quad l = K + 1, \dots, K + L, \quad (2)$$

respectively, where $\Phi \in \mathbb{C}^{M \times M}$ is the diagonal phase-shifter matrix having $\Phi(m, m) = \beta_m \phi_m$ for $\forall m = 1, 2, \dots, M$ and $\mathbf{f}_i \in \mathbb{C}^{N_t \times 1}$ for $\forall i = 1, 2, \dots, K$ is the active transmit beamformer towards DU_i , while $\mathbf{F}_E \in \mathbb{C}^{N_t \times N_t}$ is an energy precoding matrix. Note that $\beta_m \in [0, 1]$, for $\forall m = 1, 2, \dots, M$ is the amplitude reflection coefficient of the m -th passive reflector. We assume that $\beta_m = 1$ for $\forall m$, while n_i , for $\forall i = 1, 2, \dots, K + L$ is the white noise satisfying $n_i \sim \mathcal{CN}(0, \sigma^2)$.

The achievable rate of DU_k is expressed as

$$r_k = \log \left(1 + \frac{\|(\mathbf{h}_{d,k}^H + \mathbf{g}_k^H \Phi \mathbf{H}_r) \mathbf{f}_k\|^2}{I_k + \sigma^2} \right), \quad (3)$$

where $I_k = \sum_{i \neq k} \|(\mathbf{h}_{d,k}^H + \mathbf{g}_k^H \Phi \mathbf{H}_r) \mathbf{f}_i\|^2 + \|(\mathbf{h}_{d,k}^H + \mathbf{g}_k^H \Phi \mathbf{H}_r) \mathbf{F}_E\|^2$, while the received RF power of EU_l is expressed as

$$E_l^{RF} = \sum_{i=1}^K \|(\mathbf{h}_{d,l}^H + \mathbf{g}_l^H \Phi \mathbf{H}_r) \mathbf{f}_i\|^2 + \|(\mathbf{h}_{d,l}^H + \mathbf{g}_l^H \Phi \mathbf{H}_r) \mathbf{F}_E\|^2. \quad (4)$$

Discussion: The transmitter broadcasts the data symbols $\mathbf{s} = [s_1, s_2, \dots, s_K]$ to all users, where s_i is a 1×1 M-QAM modulated symbol satisfying $\mathbb{E}(s_i) = 1$. The k -th user receives both the RF signal directly from the transmitter and that reflected by the IRS, which are then expressed as

$$y_k = (\mathbf{h}_{d,k} + \mathbf{g}_k \Phi \mathbf{H}_r) \left(\sum_{i=1}^K \mathbf{f}_i s_i + \mathbf{F}_E \mathbf{s}_E \right) + n_k, \quad k = 1, \dots, K, \quad (5)$$

When the SINR is low, the receiver may not detect the received signal with low bit-error rate. [34] investigates the

achievable rate in IDET system with discrete transmitted symbol, while the achievable rate of DU_k is expressed as

$$r_k = \log_2 M - \frac{1}{M} \sum_{x \in \chi} \log_2 [1 + (M-1) \times \exp(-\frac{\gamma}{M-1} \sum_{x' \in \chi, x' \neq x} |x - x'|^2)], \quad (6)$$

where χ is the set of all the modulated symbols, and x is any symbol in χ .

Observe from Eq. (6) that the SINR results in a higher achievable rate. Therefore, we reformulate the constraint of the achievable rate on DU_k to that of the SINR constraints. Further, the beamformer at the transmitter and the IRS is readily obtained with the aid of the STMO algorithm.

According to [21], [35], [36], the channel estimations of the direct channels from the transmitter to the users is much more accurate than that of the IRS cascaded channels. This is because the IRS has no RF chains and the number of reflectors in the IRS is far larger than the number of antennas in the transmitter, which results insufficient degree of freedom for channel estimation. Therefore, we assume that the CSI of the cascaded transmitter-IRS-user channel is imperfect. According to [21], the IRS cascaded channels is estimated as $\text{diag}(\hat{\mathbf{g}}_l^H) \hat{\mathbf{H}}_r$. However, channel estimation error always exists due to the hardware and inefficient algorithm. Therefore, the relationship between the actual CSI and its estimated counterpart is modelled as

$$\text{diag}(\mathbf{g}_l^H) \mathbf{H}_r = \text{diag}(\hat{\mathbf{g}}_l^H) \hat{\mathbf{H}}_r + \Delta_l. \quad (7)$$

where Δ_l represents the channel estimation error satisfying $\|\Delta_l\|_F \leq \epsilon$.

According to [37], the saturated non-linear energy harvesting model is expressed as

$$E_l^{DC} = \Psi(E_l^{RF}) = \frac{E_{\max}^{DC}}{X(1 + \exp(-a(E_l^{RF} - b)))} - Y, [Watt] \quad (8)$$

where E_l^{RF} is the input RF power and E_l^{DC} is the output DC power. $X = \frac{\exp(ab)}{1 + \exp(ab)}$ and $Y = \frac{E_{\max}^{DC}}{\exp(ab)}$ are constants, where a and b represent the joint impact of the resistances, the capacitances, and the circuit sensitivity on the rectifying process. Denote that E_{\max}^{DC} represents the saturated upper-bound of the output DC power.

III. PROBLEM FORMULATION AND ALGORITHM

Our goal is to minimize the total transmit power at the transmitter by jointly designing the transmit beamformers $\{\mathbf{f}_1, \dots, \mathbf{f}_K, \mathbf{F}_E\}$ of the transmitter and the passive reflecting beamformer Φ of the IRS. This problem is formulated as

$$(P1): \min_{\mathbf{f}_1, \dots, \mathbf{f}_K, \mathbf{F}_E, \Phi} \sum_{i=1}^K \|\mathbf{f}_i\|^2 + \|\mathbf{F}_E\|^2, \quad (9)$$

$$\text{s.t. } r_k \geq r_0, \quad \forall \Delta_k, k = 1, 2, \dots, K, \quad (9a)$$

$$E_l^{DC} \geq E_0, \quad \forall \Delta_l, l = K+1, \dots, K+L, \quad (9b)$$

$$\|\Delta_i\|_F < \epsilon, \quad i = 1, 2, \dots, K+L, \quad (9c)$$

$$|\Phi(m, m)|^2 = 1, \quad m = 1, 2, \dots, M, \quad (9d)$$

where the WDT requirements of the DUs and the WET requirements of the EUs are expressed in (9a) and (9b), respectively. Moreover, (9c) represents that the channel estimation error Δ_i is upper-bounded, while (9d) illustrates the norm constraints on the passive reflecting beamformer of the IRS. Unfortunately, (P1) is difficult to solve, because we are uncertain about the exact value of the channel estimation error Δ_i and the energy harvesting function is non-linear.

By considering the monotonically increasing property between the input RF power and output DC power, we may replace the DC power constraints of Eq. (9b) by the RF power constraints of Eq. (10b). Furthermore, a higher signal-interference-plus-noise ratio (SINR) results in a higher achievable rate. Therefore, (P1) can be equivalently reformulated as

$$(P1.1): \min_{\mathbf{f}_1, \dots, \mathbf{f}_K, \mathbf{F}_E, \Phi} \sum_{i=1}^K \|\mathbf{f}_i\|^2 + \|\mathbf{F}_E\|^2, \quad (10)$$

$$\text{s.t. } \gamma_k \geq \gamma_0, \quad \forall \Delta_k, k = 1, 2, \dots, K, \quad (10a)$$

$$E_l^{RF} \geq E_0^{RF}, \quad \forall \Delta_l, l = K+1, K+2, \dots, K+L, \quad (10b)$$

$$\text{Eq.(9c), Eq.(9d)}$$

where $\gamma_k = \frac{\|(\mathbf{h}_{d,k}^H + \mathbf{g}_k^H \Phi \mathbf{H}_r) \mathbf{f}_k\|^2}{I_k + \sigma^2}$ for $\forall k = 1, \dots, K$, while γ_0 satisfies $\log(1 + \gamma_0) = r_0$ and E_0^{RF} satisfies $\Psi(E_0^{RF}) = E_0$.

Therefore, in order to always satisfy the WDT and WET requirements, a robust design is adopted for combating all possible channel estimation errors, even the worst one.

Lemma 1 [38] is introduced to solve the uncertainties of the channel estimation error.

Lemma 1: {S-Procedure} Consider the following two quadratic functions

$$h_1(\mathbf{x}) = \mathbf{x}^H \mathbf{A}_1 \mathbf{x} + \mathbf{x}^H \mathbf{b}_1 + \mathbf{b}_1^H \mathbf{x} + c_1, \quad (11)$$

$$h_2(\mathbf{x}) = \mathbf{x}^H \mathbf{A}_2 \mathbf{x} + \mathbf{x}^H \mathbf{b}_2 + \mathbf{b}_2^H \mathbf{x} + c_2, \quad (12)$$

where $\mathbf{x} \in \mathbb{C}^{N_t \times 1}$, and $\mathbf{A}_1, \mathbf{A}_2 \in \mathbb{C}^{N_t \times N_t}$ are complex Hermitian matrices. The following two conditions are equivalent to each other:

- $h_2(\bar{\mathbf{x}}) \leq 0$ for all $\bar{\mathbf{x}}$ satisfying $h_1(\bar{\mathbf{x}}) \neq 0$;
- There exists a $\lambda \leq 0$ such that

$$\begin{bmatrix} \mathbf{A}_2 & \mathbf{b}_2 \\ \mathbf{b}_2^H & c_2 \end{bmatrix} + \lambda \begin{bmatrix} \mathbf{A}_1 & \mathbf{b}_1 \\ \mathbf{b}_1^H & c_1 \end{bmatrix} \succeq 0. \quad (13)$$

Proof: Please refer to [38] for more details. ■

Lemma 2: Constraints (10a) in (P1.1) can be rewritten as $\text{vec}(\Delta)^H \mathbf{A}_k \text{vec}(\Delta) + \mathbf{b}_k^H \text{vec}(\Delta) + \text{vec}(\Delta)^H \mathbf{b}_k + c_k > 0$ (14)

where we have

$$\mathbf{A}_k = (\mathbf{f}_k \mathbf{f}_k^H - \gamma_0 (\sum_{j \neq k} \mathbf{f}_j \mathbf{f}_j^H + \mathbf{F}_E \mathbf{F}_E^H)) \otimes (\text{vec}(\Phi) \text{vec}(\Phi)^H),$$

$$\mathbf{b}_k = \text{vec}(\text{vec}(\Phi)^H (\mathbf{h}_{d,k}^H + \text{vec}(\Phi)^H \text{diag}(\hat{\mathbf{g}}_k^H) \hat{\mathbf{H}}_r)) (\mathbf{f}_k \mathbf{f}_k^H - \gamma_0 (\sum_{j \neq k} \mathbf{f}_j \mathbf{f}_j^H + \mathbf{F}_E \mathbf{F}_E^H)),$$

$$c_k = (\mathbf{h}_{d,k}^H + \text{vec}(\Phi)^H \text{diag}(\hat{\mathbf{g}}_k^H) \hat{\mathbf{H}}_r) (\mathbf{f}_k \mathbf{f}_k^H - \gamma_0 (\sum_{j \neq k} \mathbf{f}_j \mathbf{f}_j^H + \mathbf{F}_E \mathbf{F}_E^H)) (\mathbf{h}_{d,k}^H + \text{vec}(\Phi)^H \text{diag}(\hat{\mathbf{g}}_k^H) \hat{\mathbf{H}}_r)^H - \gamma_0 \sigma_2.$$

Proof: Please refer to Appendix A for more details. ■

Therefore, by adopting *Lemma 1* and *Lemma 2*, constraints (10a) are equivalent to

$$\begin{bmatrix} \mathbf{A}_k + \lambda_k \mathbf{I} & \mathbf{b}_k \\ \mathbf{b}_k^H & c_k - \lambda_k \epsilon \end{bmatrix} \succeq 0, \forall k = 1, 2, \dots, K. \quad (15)$$

Similarly, according to *Lemma 1* and *Lemma 2*, constraints (9c) are equivalent to

$$\begin{bmatrix} \mathbf{A}_l + \lambda_l \mathbf{I} & \mathbf{b}_l \\ \mathbf{b}_l^H & c_l - \lambda_l \epsilon \end{bmatrix} \succeq 0, \forall l = K + 1, K + 2, \dots, K + L. \quad (16)$$

where we have

$$\begin{aligned} \mathbf{A}_l &= \left(\sum_{j=1}^K \mathbf{f}_j \mathbf{f}_j^H + \mathbf{F}_E \mathbf{F}_E^H \right) \otimes (\text{vec}(\Phi) \text{vec}(\Phi)^H), \\ \mathbf{b}_l &= \text{vec}(\text{vec}(\Phi)^H (\mathbf{h}_{d,k}^H + \text{vec}(\Phi)^H \text{diag}(\hat{\mathbf{g}}_k^H) \hat{\mathbf{H}}_r)) \\ &\quad \times \left(\sum_{j=1}^K \mathbf{f}_j \mathbf{f}_j^H + \mathbf{F}_E \mathbf{F}_E^H \right)^H, \\ c_l &= (\mathbf{h}_{d,k}^H + \text{vec}(\Phi)^H \text{diag}(\hat{\mathbf{g}}_k^H) \hat{\mathbf{H}}_r) \left(\sum_{j=1}^K \mathbf{f}_j \mathbf{f}_j^H + \mathbf{F}_E \mathbf{F}_E^H \right) \\ &\quad (\mathbf{h}_{d,k}^H + \text{vec}(\Phi)^H \text{diag}(\hat{\mathbf{g}}_k^H) \hat{\mathbf{H}}_r)^H - E_0^{RF}. \end{aligned}$$

As a result, (P1.1) can be reformulated as

$$(P1.2): \min_{\mathbf{f}_1, \dots, \mathbf{f}_K, \mathbf{F}_E, \Phi} \sum_{i=1}^K \|\mathbf{f}_i\|^2 + \|\mathbf{F}_E\|^2, \quad (17)$$

$$\text{s.t.} \begin{bmatrix} \mathbf{A}_k + \lambda_k \mathbf{I} & \mathbf{b}_k \\ \mathbf{b}_k^H & c_k - \lambda_k \epsilon \end{bmatrix} \succeq 0, \forall k = 1, 2, \dots, K, \quad (17a)$$

$$\begin{bmatrix} \mathbf{A}_l + \lambda_l \mathbf{I} & \mathbf{b}_l \\ \mathbf{b}_l^H & c_l - \lambda_l \epsilon \end{bmatrix} \succeq 0, \forall l = K + 1, \dots, K + L, \quad (17b)$$

$$|\Phi(m, m)|^2 = 1, \forall m = 1, 2, \dots, M, \quad (17c)$$

$$\lambda_i \geq 0, \forall i = 1, 2, \dots, K + L. \quad (17d)$$

A. Transmit Covariance Design with Fixed Reflecting Beamformer

Let us denote the transmit covariance as $\mathbf{S}_i = \mathbf{f}_i \mathbf{f}_i^H$ and $\mathbf{S}_E = \mathbf{F}_E \mathbf{F}_E^H$. When we fix the passive reflecting beamformer of the IRS, (P1.2) can be converted to

$$(P2): \min_{\mathbf{S}_1, \dots, \mathbf{S}_K, \mathbf{S}_E} \text{Trace} \left(\sum_{i=1}^K \mathbf{S}_i + \mathbf{S}_E \right), \quad (18)$$

$$\text{s.t.} \lambda_i \geq 0, i = 1, 2, \dots, K + L. \quad (18a)$$

$$\mathbf{S}_i \succeq 0, i = 1, 2, \dots, K \quad (18b)$$

$$\mathbf{S}_E \succeq 0. \quad (18c)$$

$$\text{rank}(\mathbf{S}_i) = 1, i = 1, 2, \dots, K \quad (18d)$$

$$\text{Eq.}(17a), \text{Eq.}(17b).$$

By relaxing the rank-one constraints of Eq. (18c), (P2) is reformulated as

$$(P2.1): \min_{\mathbf{S}_1, \dots, \mathbf{S}_K, \mathbf{S}_E} \text{Trace} \left(\sum_{i=1}^K \mathbf{S}_i + \mathbf{S}_E \right), \quad (19)$$

$$\text{s.t.} \text{Eq.}(17a), \text{Eq.}(17b), \text{Eq.}(18a) - \text{Eq.}(18c)$$

Note that \mathbf{A}_i , \mathbf{b}_i and c_i for $\forall i = 1, 2, \dots, K + L$ are linear with respect to $\{\mathbf{S}_1, \dots, \mathbf{S}_K, \mathbf{S}_E\}$. This problem is a convex problem, which can be solved by a standard toolbox.

B. Reflecting Beamformer Design with fixed Covariance Matrices

When $\{\mathbf{S}_1, \dots, \mathbf{S}_K, \mathbf{S}_E\}$ are fixed, the value of the objective function in (P1.1) is a constant. We can optimize the passive reflecting beamformer Φ to potentially improve the WDT and WET performance. The attainable WDT and WET performance are thus much higher than the original requirements. When we optimize the covariance matrices based on the passive reflecting beamformer Φ in next iteration, we can further reduce the transmit power due to the performance overflow. Here, we try to improve the WET performance, while satisfying the WDT requirements. Our goal is to maximize the lower-bound of all the EUs' WET performance. The problem is then formulated as

$$(P3): \max_{\Phi} E^{RF}, \quad (20)$$

$$\text{s.t.} \text{Eq.}(9a) - \text{Eq.}(9d).$$

However, the constraint (9a) is non-convex with respect to the passive reflecting beamformer Φ . In order to solve this problem, we have the following proposition:

Proposition 1: The necessary conditions of constraints (9a) are expressed as

$$\begin{bmatrix} \mathbf{A}'_k + \mu_k \mathbf{I} & \mathbf{b}'_k \\ \mathbf{b}'_k{}^H & c'_k - \mu_k \epsilon \end{bmatrix} \succeq 0, k = 1, 2, \dots, K, \quad (21)$$

where we have

$$\begin{aligned} \mathbf{A}'_k &= (\mathbf{S}_k - \gamma_0 \left(\sum_{i \neq k} \mathbf{S}_i + \mathbf{S}_E \right)) \otimes (\text{vec}(\Phi) \text{vec}(\Phi)^H)^H \\ &\quad + \text{vec}(\Phi^{[n]}) \text{vec}(\Phi)^H - \text{vec}(\Phi^{[n]}) \text{vec}(\Phi^{[n]})^H \\ \mathbf{b}'_k &= [\text{vec}(\text{vec}(\Phi^{[n]})^H (\mathbf{h}_{d,k}^H + \text{vec}(\Phi)^H \text{diag}(\hat{\mathbf{g}}_k^H) \hat{\mathbf{H}}_r)) + \\ &\quad \text{vec}(\text{vec}(\Phi)^H (\mathbf{h}_{d,k}^H + \text{vec}(\Phi^{[n]})^H \text{diag}(\hat{\mathbf{g}}_k^H) \hat{\mathbf{H}}_r)) - \text{vec}(\text{vec}(\Phi^{[n]}) \\ &\quad \text{vec}(\Phi^{[n]}) (\mathbf{h}_{d,k}^H + \text{vec}(\Phi^{[n]}) \text{diag}(\hat{\mathbf{g}}_k^H) \hat{\mathbf{H}}_r))] (\mathbf{S}_k - \gamma_0 \left(\sum_{i \neq k} \mathbf{S}_i + \mathbf{S}_E \right)) \\ c'_k &= 2\text{Re}[(\mathbf{h}_{d,k}^H + \text{vec}(\Phi^{[n]}) \text{diag}(\hat{\mathbf{g}}_k^H) \hat{\mathbf{H}}_r) \\ &\quad (\mathbf{S}_k - \gamma_0 \left(\sum_{i \neq k} \mathbf{S}_i + \mathbf{S}_E \right)) (\mathbf{h}_{d,k}^H + \text{vec}(\Phi) \text{diag}(\hat{\mathbf{g}}_k^H) \\ &\quad \hat{\mathbf{H}}_r)^H] - (\mathbf{h}_{d,k}^H + \text{diag}(\hat{\mathbf{g}}_k^H) \hat{\mathbf{H}}_r) (\mathbf{S}_k - \gamma_0 \left(\sum_{i \neq k} \mathbf{S}_i + \mathbf{S}_E \right)) \\ &\quad (\mathbf{h}_{d,k}^H + \text{vec}(\Phi^{[n]}) \text{diag}(\hat{\mathbf{g}}_k^H) \hat{\mathbf{H}}_r)^H - \gamma_0 \sigma_2, \end{aligned}$$

while $\text{vec}(\Phi^{[n]})$ can take an arbitrary value and $\mu_k \geq 0$.

Proof: Please refer to Appendix B for more details. ■

Similarly, the necessary conditions of constraints (9b) are expressed as

$$\begin{bmatrix} \mathbf{A}'_l + \mu_l \mathbf{I} & \mathbf{b}'_l \\ \mathbf{b}'_l{}^H & c'_l - \mu_l \epsilon \end{bmatrix} \succeq 0, l = K + 1, \dots, K + L, \quad (22)$$

where we have

$$\begin{aligned} \mathbf{A}_l'^{[n]} &= \left(\sum_{i=1}^K \mathbf{S}_i + \mathbf{S}_E \right) \otimes (\text{vec}(\Phi) \text{vec}(\Phi^{[n]})^H + \text{vec}(\Phi^{[n]}) \\ &\text{vec}(\Phi)^H - \text{vec}(\Phi^{[n]}) \text{vec}(\Phi^{[n]})^H) \\ \mathbf{b}_l'^{[n]} &= [\text{vec}(\text{vec}(\Phi^{[n]})^H (\mathbf{h}_{d,k}^H + \text{vec}(\Phi)^H \text{diag}(\hat{\mathbf{g}}_k^H) \hat{\mathbf{H}}_r)) + \\ &\text{vec}(\text{vec}(\Phi)^H (\mathbf{h}_{d,k}^H + \text{vec}(\Phi^{[n]})^H \text{diag}(\hat{\mathbf{g}}_k^H) \hat{\mathbf{H}}_r)) \text{vec}(\text{vec}(\Phi^{[n]})^H (\mathbf{h}_{d,k}^H + \text{vec}(\Phi^{[n]})^H \text{diag}(\hat{\mathbf{g}}_k^H) \hat{\mathbf{H}}_r))] \left(\sum_{i=1}^K \mathbf{S}_i + \mathbf{S}_E \right) \\ \mathbf{c}_l'^{[n]} &= 2\text{Re}[(\mathbf{h}_{d,k}^H + \text{vec}(\Phi^{[n]})^H \text{diag}(\hat{\mathbf{g}}_k^H) \hat{\mathbf{H}}_r) \left(\sum_{i=1}^K \mathbf{S}_i + \mathbf{S}_E \right) \\ &(\mathbf{h}_{d,k}^H + \text{vec}(\Phi)^H \text{diag}(\hat{\mathbf{g}}_k^H) \hat{\mathbf{H}}_r)^H] - (\mathbf{h}_{d,k}^H + \text{vec}(\Phi^{[n]})^H \text{diag} \\ &(\hat{\mathbf{g}}_k^H) \hat{\mathbf{H}}_r) \left(\sum_{i=1}^K \mathbf{S}_i + \mathbf{S}_E \right) (\mathbf{h}_{d,k}^H + \text{vec}(\Phi^{[n]})^H \text{diag}(\hat{\mathbf{g}}_k^H) \hat{\mathbf{H}}_r)^H \\ &- E^{RF}, \end{aligned}$$

while $\text{vec}(\Phi^{[n]})$ can take an arbitrary value and $\mu_l \geq 0$.

The constraints (9d) on phase shifters are reformulated as $1 \leq |\Phi(m, m)|^2 \leq 1$, in which the non-convex part is $1 \leq |\Phi(m, m)|^2$. By adding slack variables $v_i \geq 0$ for $\forall i = 1, 2, \dots, 2M$, the linearized form of the non-convex constraints are expressed as $2\Re(\Phi(m, m)^H \Phi(m, m)^{[n]}) - |\Phi(m, m)^{[n]}|^2 - v_m \geq 1$ with any fixed $\Phi(m, m)^{[n]}$. According to *Proposition 1* and *Lemma 1*, given an arbitrary passive reflecting beamformer $\Phi^{[0]}$, (P3) is reformulated as

$$(P3.1): \max_{\Phi, v_1, \dots, v_{2M}} E^{RF} - \delta^{[n]} \sum_{i=1}^{2M} v_i, \quad (23)$$

$$\text{s.t.} \begin{bmatrix} \mathbf{A}_k'^{[0]} + \mu_k \mathbf{I} & \mathbf{b}_k'^{[0]} \\ \mathbf{b}_k'^{[0]H} & c_k'^{[0]} - \mu_k \epsilon, \end{bmatrix} \succeq 0, \quad k = 1, 2, \dots, K + L, \quad (23a)$$

$$\mu_i \geq 0 \quad i = 1, 2, \dots, K + L, \quad (23b)$$

$$2\Re(\Phi(m, m)^H \Phi(m, m)^{[n]}) - |\Phi(m, m)^{[n]}|^2 - v_m \geq 1, \quad m = 1, 2, \dots, M, \quad (23c)$$

$$|\Phi(m, m)|^2 \leq 1 + v_{M+m}, \quad m = 1, 2, \dots, M, \quad (23d)$$

$$v_i \geq 0, \quad i = 1, 2, \dots, M, \quad (23e)$$

where $\delta^{[n]} > 0$ is regularization factor. In (P3.1), we add the slack variables v_i and $\delta^{[n]}$, the unit constraint $1 \leq |\Phi(m, m)|^2 \leq 1$ is converted to the convex constraints, which is expressed as

$$2\Re(\Phi(m, m)^H \Phi(m, m)^{[n]}) - |\Phi(m, m)^{[n]}|^2 + v_m \geq 1, \quad m = 1, 2, \dots, M, \quad (24)$$

$$|\Phi(m, m)|^2 \leq 1 + v_{M+m}, \quad m = 1, 2, \dots, M, \quad (25)$$

where $\Phi(m, m)^{[n]}$ is the solution of the previous iteration. In (P3), our goal is to maximize the received energy by satisfying the norm constraints of $\Phi(m, m)$. By introducing the slack variables, the objective function is reformulated as

$$E^{RF} - \delta^{[n]} \sum_{i=1}^{2M} v_i, \quad (26)$$

Algorithm 1 Phase-shifters of the IRS Design

Input: The channels \mathbf{H}_r , $\{\mathbf{g}_r\}$, $\{\mathbf{g}_{d,l}\}$ and $\{\mathbf{h}_k\}$, $\{\mathbf{h}_{d,k}\}$; the transmit covariance matrices $\{\mathbf{S}_1^n, \dots, \mathbf{S}_K^n, \mathbf{S}_E^n\}$. initialization of the passive reflecting beamformer $\text{vec}(\Phi_c^{[0]})$ of the IRS; error tolerance ϵ ; $P^1 = 0$; $n = 0$;

Output: The phase-shifter $\text{vec}(\Phi)^*$ of the IRS;

```

1: while ( $\nu > \epsilon$ ) do
2:    $n \leftarrow n + 1$ ;
3:    $P^0 \leftarrow P^1$ ;
4:   Obtain the the phase-shifters  $\text{vec}(\Phi^{[n]})$  of the IRS and objective value  $E_n^{RF}$  by solving (P3.1);
5:    $P^1 \leftarrow E_n^{RF}$ ;
6:    $\nu \leftarrow ||P^1 - P^0||$ ;
7: end while
8: return  $\text{vec}(\Phi^*) \leftarrow \text{vec}(\Phi^{[n]})$ .

```

When $\Phi(m, m)$ is smaller than 1, we have $2\Re(\Phi(m, m)^H \Phi(m, m)^{[n]}) - |\Phi(m, m)^{[n]}|^2 < 1$ in constraints Eq.(24). Therefore, the slack variable $v_m > 0$ should satisfy the constraints Eq.(24), which may reduce the objective function value. According to Eq.(25), when the norm of $\Phi(m, m)$ is larger than 1, we have $v_{M+m} > 0$, which also reduces the objective function value. As a result, the slack variables v_i and $\delta^{[n]}$ reinforce the unit constraints on $\Phi(m, m)$ holding on. Moreover, denoting Φ^* as the optimal solution to (P3) satisfying the unit constraints, Φ^* is also optimal to (P3.1), since Φ^* maximizes E^{RF} and the slack variables could be 0. Therefore, the relaxed optimization problem has the same optimal solution as the original one.

Note that (P3.1) is a convex problem. Denote the optimal solution to (P3.1) as $\Phi^{[1]}$. We define an auxiliary function $E^{RF}(\Phi^{[0]}|\Phi^{[1]})$ as the objective value of (P3.1), where $\Phi^{[0]}$ is the given passive beamformer and $\Phi^{[1]}$ is the optimal solution. We have $E^{RF}(\Phi^{[0]}|\Phi^{[0]}) < E^{RF}(\Phi^{[0]}|\Phi^{[1]})$, since $\Phi^{[1]}$ is the optimal solution to (P3.1). Furthermore, we have $E^{RF}(\Phi^{[1]}|\Phi^{[1]}) > E^{RF}(\Phi^{[0]}|\Phi^{[1]})$ due to the triangle inequality. As a result, by initialising $\text{vec}(\Phi^{[0]})$, we may sequentially obtain $\text{vec}(\Phi^{[0]})$, $\text{vec}(\Phi^{[1]})$, \dots , $\text{vec}(\Phi^{[n]})$, \dots . When n is sufficiently large, the objective of (P3.1) converges. The corresponding solution can be regarded as the local optimal solution, i.e. $\text{vec}(\Phi^*) = \text{vec}(\Phi^{[n]})$ to (P3). When we optimize (P3.1) in n -th iteration, $\delta^{[n]}$ is not a variable.

$$\delta^{[n]} = \begin{cases} \lambda \delta^{[n-1]} & \text{if } \delta^{[n]} < \delta^{max} \\ \delta^{max} & \text{else} \end{cases} \quad (27)$$

where $\lambda > 1$ and $\delta^0 > 0$. When $\delta^{[n]}$ is large and the solution does not satisfy constrain (7d), the objective function value will reduce rapidly. The main steps for solving (P3) is summarised as Algorithm 1.

Convergence Analysis: Since the objective function of (P3.1) is continuous, while the constraints are continuous within closed interval, the optimum has an upper-bound. During the $(n - 1)$ -th alteration, the objective value is $E^{RF}(\Phi^{[n-1]}|\Phi^{[n-1]})$. In the next iteration, We have $E^{RF}(\Phi^{[n]}|\Phi^{[n-1]}) \geq E^{RF}(\Phi^{[n-1]}|\Phi^{[n-1]}) \geq E^{RF}(\Phi^{[n-1]}|\Phi^{[n-2]})$. Therefore, the objective value of

(P3.1) increases after every iteration. It will finally converge to a local optimal solution.

C. Joint Design

Our joint design cannot be directly solved by the classic block coordinate descent (BCD) or the alternative optimization (AO) based algorithms, since our objective function of Eq. (17) is not changed, when we optimize the passive beamformer of the IRS.

Therefore, a successive target migration optimization (STMO) based algorithm is proposed for jointly designing $\{\mathbf{S}_1, \dots, \mathbf{S}_K, \mathbf{S}_E\}$ and Φ , as detailed in Algorithm 2. In a single iteration, the transmit covariance matrices $\{\mathbf{S}_1, \dots, \mathbf{S}_K, \mathbf{S}_E\}$ are firstly optimized by solving (P2.1), as shown in Lines 4 of Algorithm 2. Then, the obtained transmit covariance matrices are substituted into (P3) for designing the reflecting beamformer Φ , as shown in Lines 5 of Algorithm 2. The iteration may be terminated, if the required accuracy is reached. The following proposition demonstrates that the iteration is effective.

Proposition 2: Denote Φ^* as the solution to problem (P3) when $\{\mathbf{S}_1, \dots, \mathbf{S}_K, \mathbf{S}_E\}$ are fixed. If the objective of (P3) satisfies $E^{RF*} > E_0^{RF}$, there exists a solution $\{\mathbf{S}'_1, \dots, \mathbf{S}'_K, \mathbf{S}'_E, \Phi^*\}$ to (P2.1) such that $Trace(\sum_{i=1}^K \mathbf{S}'_i + \mathbf{S}'_E) < Trace(\sum_{i=1}^{K+L} \mathbf{S}_i + \mathbf{S}_E)$.

Proof: Please refer to Appendix C for more details. ■

Proposition 2 demonstrates that there exists a specific group of transmit covariance matrices $\{\mathbf{S}'_1, \dots, \mathbf{S}'_K, \mathbf{S}'_E\}$ achieving lower transmit power in the next iteration, after we maximize the minimum WET performance among the EUs by optimizing the passive reflecting beamformer Φ of the IRS. Note that $\{\mathbf{S}'_1, \dots, \mathbf{S}'_K, \mathbf{S}'_E, \Phi^*\}$ given in *Proposition 2* is only a feasible solution to (P2.1). Since (P2.1) is convex, the optimal transmit covariance matrices $\{\mathbf{S}_1^*, \dots, \mathbf{S}_K^*, \mathbf{S}_E^*\}$ achieve even lower transmit power than that of the specific solution $\{\mathbf{S}'_1, \dots, \mathbf{S}'_K, \mathbf{S}'_E\}$.

The following proposition is exploited to recover a rank-one solution having the same performance as the transmit covariance matrices $\{\mathbf{S}_1, \dots, \mathbf{S}_K, \mathbf{S}_E\}$.

Proposition 3: There exists an optimal solution satisfying $rank(\mathbf{S}_i) = 1$, for $\forall i = 1, 2, \dots, K$

Proof: Please refer to Appendix D for more details. ■

Based on *Proposition 3*, we can recover the rank-one transmit WDT beamformers from the transmit covariance by eigenvalue decomposition.

Convergence Analysis: Please refer to Appendix E for more details.

Complexity Analysis: We analyze the complexity of proposed STMO algorithm. Since both (P2) and (P3) are convex problems, they can be solved by the interior point method. The general expression [39] is

$$\mathcal{O}\left(\sum_{j=1}^J b_j + 2I\right)^{1/2} n(n^2 + n \sum_{j=1}^J b_j^2 + \sum_{j=1}^J b_j^3 + n \sum_{i=1}^I a_i^2) \quad (28)$$

where n is the number of variables, J is the number of LMI (linear matrix inequality) constraints and I is the number of

Algorithm 2 STMO Algorithm For Solving (P1)

Input: The channels \mathbf{H}_r , $\{\mathbf{g}_l\}$, $\{\mathbf{g}_{d,l}\}$ and $\{\mathbf{h}_k\}$, $\{\mathbf{h}_{d,k}\}$; initialization of the passive reflecting beamformer $\text{vec}(\Phi_c^{[0]})$ of the IRS; error tolerance ε ; $P^1 = 0$; $n = 0$; Channel estimation error δ

Output: The phase of IRS Φ^* and the transmit beamformer and precoding $\{\mathbf{f}_1^*, \dots, \mathbf{f}_K^*, \mathbf{F}_E^*\}$;

- 1: **while** ($\nu > \varepsilon$) **do**
- 2: $n \leftarrow n + 1$;
- 3: $P^0 \leftarrow P^1$;
- 4: Obtain the transmit covariance matrices $\{\mathbf{S}_1^n, \dots, \mathbf{S}_K^n, \mathbf{S}_E^n\}$ by solving (P2.1);
- 5: Obtain the continues phase of IRS Φ^n by substituting $\{\mathbf{S}_1^n, \dots, \mathbf{S}_K^n, \mathbf{S}_E^n\}$ into Algorithm 1;
- 6: $P^1 \leftarrow Trace(\sum_{i=1}^K \mathbf{S}_i^n + \mathbf{S}_E^n)$;
- 7: $\nu \leftarrow ||P^1 - P^0||$;
- 8: **end while**
- 9: Obtain the $\{\mathbf{f}_1^*, \dots, \mathbf{f}_K^*, \mathbf{F}_E^*\}$ according to Proposition 3;
- 10: **return** $\{\mathbf{f}_1^*, \dots, \mathbf{f}_K^*, \mathbf{F}_E^*$ and $\Phi^n\}$.

SOC (second-order cone) constraints. The size of j -th LMI constraint is b_j , while the size of i -th SOC constraint is a_i .

(P2.1) is solved by semi-definite program, the complexity of which is $\mathcal{O}((K+L)(N_t M)^{1/2}(K+1)N_t^2((K+1)^2 N_t^4 + (K+1)(K+L)N_t^4 M^2 + (K+L)N_t^3 M^3))$. (P3) is solved by Algorithm 1, the complexity of which is $\mathcal{O}((K+L)N_t M + 2M)^{1/2} M(M^2 + (K+L)N_t^2 M^3 + (K+L)N_t^3 M^3 + M^2)I_{iter1}$, where I_{iter1} is the number of iteration in Algorithm 1. The total complexity is $\mathcal{O}([(K+L)(N_t M)^{1/2}(K+1)N_t^2((K+1)^2 N_t^4 + (K+1)(K+L)N_t^4 M^2 + (K+L)N_t^3 M^3) + (K+L)N_t M + 2M]^{1/2} M(M^2 + (K+L)N_t^2 M^3 + (K+L)N_t^3 M^3 + M^2)I_{iter1}]I_{iter2})$, where I_{iter2} is the number of iteration in Algorithm 2.

IV. NUMERICAL RESULT

We assume a 2-D linear antenna array at the IRS, which is connected to the transmitter and controlled by it. The direct channels from the transmitter to all users follow Rayleigh block fading, which is expressed as $\mathbf{h}_{d,k}(i) \sim \mathcal{CN}(0, 1)$ for $\forall i$. The channel $\mathbf{g}_{d,l}$ of EU_l has the same statistical property as $\mathbf{h}_{d,k}$. For the IRS related channels, i.e., \mathbf{H}_r , \mathbf{h}_k and \mathbf{g}_l , they obey Rician block fading. For example, \mathbf{H}_r is expressed as

$$\mathbf{H}_r = \sqrt{\frac{\beta}{\beta+1}} \mathbf{H}_r^{LOS} + \sqrt{\frac{1}{\beta+1}} \mathbf{H}_r^{NLOS}, \quad (29)$$

where β is the Rician factor, \mathbf{H}_r^{LOS} is the deterministic LOS portion and \mathbf{H}_r^{NLOS} is the non-LOS (NLOS) portion. The NLOS portion \mathbf{H}_r^{NLOS} also obeys a Rayleigh block fading. The LOS portion \mathbf{H}_r^{LOS} is further expressed as $\mathbf{H}_r^{LOS} = \mathbf{a}_r(\theta_2, \theta_1) \mathbf{a}_t(\theta_4, \theta_3)^H$, where $\mathbf{a}_r(\theta_2, \theta_1)$ is the arrival steering vector of this 2D array expressed as

$$\mathbf{a}_r(\theta_2, \theta_1) = \mathbf{a}_{az}(\theta_2, \theta_1) \otimes \mathbf{a}_{el}(\theta_2, \theta_1), \quad (30)$$

where θ_2 and θ_1 are the azimuth and elevation angles, respectively. $\mathbf{a}_{az}(\theta_2, \theta_1) \in \mathbb{C}^{M_1 \times 1}$ and $\mathbf{a}_{el}(\theta_2, \theta_1) \in \mathbb{C}^{M_2 \times 1}$ are the

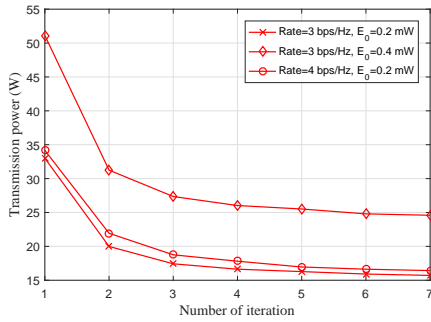


Fig. 2. Number of iterations.

uniform linear array steering vector expressed as

$$\begin{aligned} [\mathbf{a}_{az}(\theta_2, \theta_1)](n) &= e^{-j(n-1)\frac{2\pi}{\lambda}d_2\sin(\theta_2)\cos(\theta_1)}, \\ [\mathbf{a}_{el}(\theta_2, \theta_1)](n) &= e^{-j(n-1)\frac{2\pi}{\lambda}d_2\sin(\theta_2)\cos(\theta_1)}, \end{aligned} \quad (31)$$

where λ and d_1 represent the wavelength and the distance between two adjacent antennas. Furthermore, the departure steering vector $\mathbf{a}_t(\theta_4, \theta_3)$ has the same form as $\mathbf{a}_r(\theta_2, \theta_1)$, where θ_3 and θ_4 represent the azimuth and elevation angles, respectively. The wireless channel \mathbf{h}_k and \mathbf{g}_l have the same form as \mathbf{H}_r .

The transmitter is equipped with $N_t = 4$ antennas, while both EUs and DUs are equipped with a single antenna. We set 2 DUs and 2 EUs in our system. The number of reflectors in the IRS is $M = 10$. The distance from the transmitter to the IRS and that to the EUs are 1 m and 10 m, respectively, while the distance from the IRS to the EUs is 10 m. The distance from the transmitter to the DUs and that from the IRS to the DUs are 80m and 80m, respectively. The path-loss is modelled in dB as $PL = PL_0 - 10\alpha \log(d/d_0)$, where PL_0 is the path loss at the reference distance d_0 , while d denotes the signal propagation distance, and α represents the path-loss exponent. We set $d_0 = 1$ and $PL_0 = -30$ dB. The path-loss exponent of the transmitter-IRS-EU link is set to $\alpha = 2$ and that of the transmitter-EU link is set to $\alpha = 4$ [17], respectively. The Rician factor is set to 3. The noise power is -60 dBm. For the non-linear energy harvesting model of Eq. (8), we set $E_{\max}^{DC} = 24$ mW as the maximum DC power that could be output by an energy harvester. Moreover, we set $a = 150$ and $b = 0.0022$ [40]. The upper-bound of the channel estimation error is set to $\delta = 0.02$. We randomly generate $\theta_i \in [0, 2\pi], i = 1, 2, 3, 4$ in the simulation. We set $\lambda = 1.5$ and $\delta^0 = 1$ in Algorithm 2.

A. Performance of Modulated Energy Signal

Fig. 2 illustrates the convergence behavior of the proposed algorithms. We set the WDT and WET requirements to $\{3$ bps/Hz, 0.2 mW $\}$, $\{4$ bps/Hz, 0.2 mW $\}$ and $\{3$ bps/Hz, 0.4 mW $\}$, respectively. It's observed that our algorithm converges rapidly within 7 iterations.

We evaluate the transmit power against of the WDT requirements of DUs in Fig. 3. We set the WET requirements to $\{0.2$ mW, 0.4 mW $\}$, respectively. The transmit power increases as we increase the data requirements of DUs. We

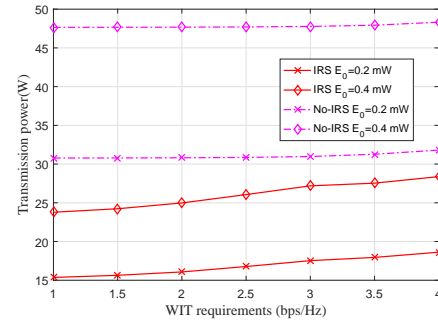


Fig. 3. Spectral efficiency VS transmit power.

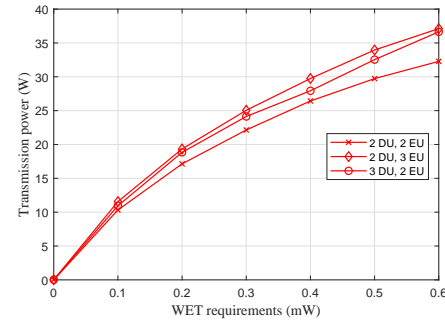


Fig. 4. Energy requirements VS transmit power.

observe from Fig. 3 that the transmit power of the IRS aided IDET system is much lower than that without an IRS. Note that no channel estimation error is assumed in the IDET system without an IRS. Therefore, the IRS can efficiently reduce the energy consumption of transmitter. Specifically, when the WET requirements of the EUs are 0.2 mW and the WDT requirements of the DUs are 3 bps/Hz, the transmit power of the IRS aided IDET system is 13.4 W lower than the counterpart without an IRS. We also observe that the transmit power increases rapidly when we increase the WET requirements. However, the transmit power increase slowly with higher WDT requirements. This is because the WET beams degrade the WDT performance. By contrast, the WDT beams can improve the WET performance. Therefore, we only need to increase the WDT power to improve the WDT performance, but we need to increase both the WDT and WET power to improve the WET performance.

We plot the transmit power versus the WET requirements of the EUs in Fig. 4. We set the WDT requirements of the DUs to 3 bps/Hz. As we expect, the transmit power increases with higher WET requirements of EUs. Specifically, when the WET requirements increase from 0.1 mW to 0.2 mW and from 0.2 mW to 0.3 mW with 2 DUs and 2 EUs, the transmit power increases by 6.8 W and 5.0 W, respectively. This is because the RF-DC conversion efficiency with an output DC power of 0.2 mW is higher than that with an output power of 0.1 mW, owing to the non-linear energy harvesting model. Therefore, we need to consume more transmit power to compensate for the low RF-DC conversion efficiency with low WET requirements. We also observe from Fig. 4 that the transmit power increases with more DUs or EUs.

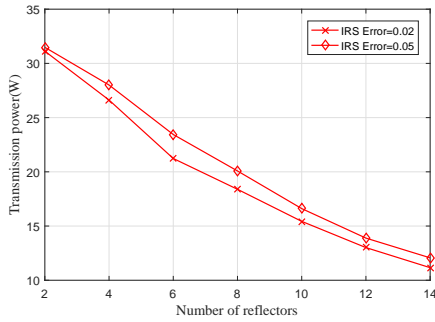


Fig. 5. Number of reflector VS transmit power.

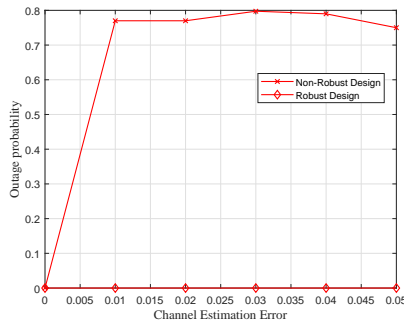


Fig. 6. Outage probability.

In Fig.5, we investigate the impact of the number of reflectors in the IRS on the transmit power. We set the WDT and WET requirements to 2 bps/Hz and 0.2 mW, respectively. Observe from Fig. 5 that the transmit power reduces if we have more reflectors in the IRS. We also observe that it requires a lower transmit power when the channel estimation error is smaller. When the number of reflectors is 2 and 10, the transmit powers under the channel estimation error $\delta = 0.02$ are 0.35 W and 0.90 W lower than that those associated with $\delta = 0.05$. The difference of transmit power is smaller between the channel estimation error $\delta = 0.02$ and $\delta = 0.05$ with 2 reflectors in the IRS. Since the number of reflectors in the IRS is small, the channel estimation error has less impact on the transmit power.

In Fig.6, we demonstrate the advantages of our robust design. The non-robust design represents that we use the estimated CSI to design the transmit beamformers and passive beamformer without considering the channel estimation error. This problem could be solved by traditional alternative optimization [15]. The outage probability is defined as the probability of at least one DU or one EU not satisfying the QoS requirements. We can observe from Fig.6 that our robust design can effectively counteract the channel uncertainty. It is quite difficult for non-robust design to satisfy the WDT requirements of 2 DUs and WET requirements of 2 EUs simultaneously. This is because when the real channel of any user is actually worse than the estimated counterpart, the non-robust design cannot satisfy the WDT and WET requirements.

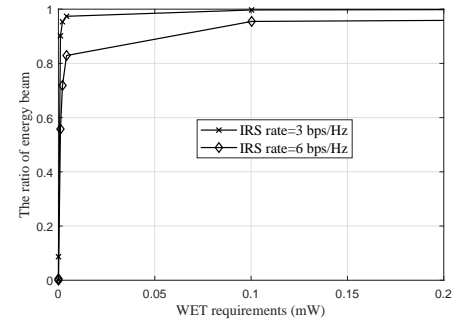


Fig. 7. The ratio of energy beam vs energy requirements.

B. Performance of Deterministic Energy Signal

When the deterministic energy signal is transmitted, the data user is able to remove the energy part from the received signal [41]. Hence, the energy beam has no interference for the data user. The achievable rate of the k -th data user is expressed as

$$r_k = \log \left(1 + \frac{\|(\mathbf{h}_{d,k}^H + \mathbf{g}_k^H \Phi \mathbf{H}_r) \mathbf{f}_k\|^2}{I_k + \sigma^2} \right), \quad (32)$$

where $I_k = \sum_{i \neq k} \|(\mathbf{h}_{d,k}^H + \mathbf{g}_k^H \Phi \mathbf{H}_r) \mathbf{f}_i\|^2$.

Our goal is to minimize the total transmit power at the transmitter by jointly designing the transmit beamformers $\{\mathbf{f}_1, \dots, \mathbf{f}_K, \mathbf{F}_E\}$ of the transmitter and the passive reflecting beamformer Φ of the IRS. This problem is formulated as

$$(P4): \min_{\mathbf{f}_1, \dots, \mathbf{f}_K, \mathbf{F}_E, \Phi} \sum_{i=1}^K \|\mathbf{f}_i\|^2 + \|\mathbf{F}_E\|^2, \quad (33)$$

$$\text{s.t. } r_k \geq r_0, \quad \forall \Delta_k, k = 1, 2, \dots, K, \quad (33a)$$

$$E_l^{DC} \geq E_0, \quad \forall \Delta_l, l = K + 1, \dots, K + L, \quad (33b)$$

$$\|\Delta_i\|_F < \epsilon, \quad i = 1, 2, \dots, K + L, \quad (33c)$$

$$|\Phi(m, m)|^2 = 1, \quad m = 1, 2, \dots, M, \quad (33d)$$

(P4) is similar to (P1) in the manuscript. Therefore, (P4) could also be solved by the STMO algorithm in Section III.

We investigate the impact of the ratio of energy beam in the IDET when the transmitter adopts the deterministic energy signal (DES) in Fig.7. We observe that the ratio of energy beam increases, when we increase the energy requirements. This is because the energy beam is targeted to the energy user, while it does not cause any interference for the data user. Therefore, the transmitter is able to increase the power of the energy beam, in order to satisfy the energy requirements.

We investigate the impact of the two energy signals, where 'DES' and 'MES' represent the deterministic energy signal and modulated energy signal, respectively. Observe from Fig 8 that the transmit power by adopting DES is lower than that of MES. This is because the energy beam has no interference to the data user, while it is capable of targeting to the energy user by adopting DES. On the contrary, the MES energy beam causes extra interference to data users. Therefore, the power of the MES energy beam tends to be zero. In order to satisfying the energy requirements of energy users, the data beam scattering with a low WET efficiency is relied upon.

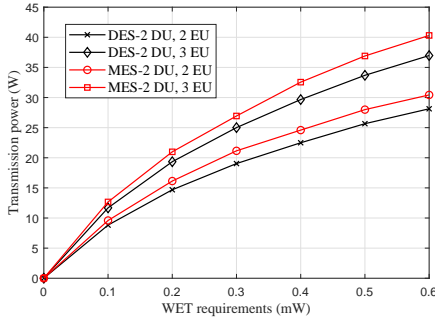


Fig. 8. The comparison of two energy signals.

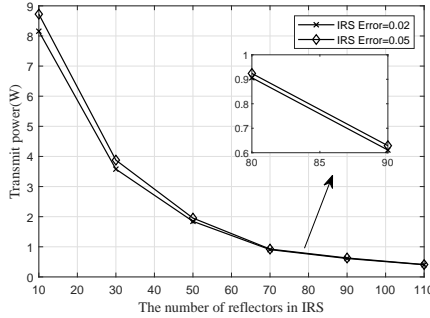


Fig. 9. The impact on number of reflectors in IRS.

Therefore, the transmit power by adopting DES is lower than that of MES.

In Fig.9, we investigate the impact of the number of reflectors in the IRS on the transmit power. We set the WDT and WET requirements to 2 bps/Hz and 0.2 mW, respectively. Observe from Fig. 9 that the transmit power reduces if we have more reflectors in the IRS. Furthermore, when the number of reflectors in the IRS increases, the the difference of transmit power become smaller between the channel estimation error $\delta = 0.02$ and $\delta = 0.05$.

V. CONCLUSION

In this paper, we study a robust design in an IRS aided MISO-IDET system by considering the imperfect channel estimation. We jointly design the transmit beamformer and the passive reflecting beamformer of the IRS in order to minimize the transmit power, while satisfying both the WDT and WET requirements constraints. A STMO algorithm is proposed for solving the non-convex problem. A number of numerical results characterize the advantages of our design. When the WDT and WET requirements are set to 3 bps/Hz and 0.2 mW. the transmit power of the IRS aided system is 13.4 W lower than the counterpart without the IRS. This demonstrates that implementing the IRS is capable of substantially reducing the energy consumption of the transmitter.

APPENDIX A PROOF OF LEMMA 2

We observe that both numerators and denominators in Eq.(10a) have the quadratic term $\mathbf{h}_{d,k} + \mathbf{g}_k \Phi \mathbf{H}_r$. Therefore,

we can covert them into one quadratic term, which is expressed as

$$\frac{\|(\mathbf{h}_{d,k} + \mathbf{g}_k \Phi \mathbf{H}_r) \mathbf{f}_k\|^2}{I_k + \sigma^2} > \gamma_0, \quad (34)$$

$$\Leftrightarrow (\mathbf{h}_{d,k} + \text{vec}(\Phi) \text{diag}(\mathbf{g}_k) \mathbf{H}_r) (\mathbf{f}_k \mathbf{f}_k^H - \gamma_0 \sum_{i \neq k} (\mathbf{f}_i \mathbf{f}_i^H + \mathbf{F}_E \mathbf{F}_E^H)) (\mathbf{h}_{d,k} + \text{vec}(\Phi) \text{diag}(\mathbf{g}_k) \mathbf{H}_r)^H - \gamma_0 \sigma^2 > 0.$$

By substituting $\text{diag}(\mathbf{g}_k) \mathbf{H}_r = \text{diag}(\hat{\mathbf{g}}_k) \hat{\mathbf{H}}_r + \Delta$ into Eq (34), it can be derived as

$$\begin{aligned} & \{ \mathbf{h}_{d,k} + \text{vec}(\Phi) [\text{diag}(\hat{\mathbf{g}}_k) \hat{\mathbf{H}}_r + \Delta] \} (\mathbf{f}_k \mathbf{f}_k^H - \gamma_0 \sum_{i \neq k} (\mathbf{f}_i \mathbf{f}_i^H + \mathbf{F}_E \mathbf{F}_E^H)) \{ \mathbf{h}_{d,k} + \text{vec}(\Phi) [\text{diag}(\hat{\mathbf{g}}_k) \hat{\mathbf{H}}_r + \Delta] \}^H - \gamma_0 \sigma^2 > 0 \\ \Leftrightarrow & \text{vec}(\Phi) \Delta (\mathbf{f}_k \mathbf{f}_k^H - \gamma_0 \sum_{i \neq k} (\mathbf{f}_i \mathbf{f}_i^H + \mathbf{F}_E \mathbf{F}_E^H)) \Delta^H \text{vec}(\Phi) \\ & + \text{vec}(\Phi) \Delta (\mathbf{f}_k \mathbf{f}_k^H - \gamma_0 \sum_{i \neq k} (\mathbf{f}_i \mathbf{f}_i^H + \mathbf{F}_E \mathbf{F}_E^H)) (\mathbf{h}_{d,k} + \text{vec}(\Phi) \text{diag}(\hat{\mathbf{g}}_k) \hat{\mathbf{H}}_r)^H \\ & + (\mathbf{h}_{d,k} + \text{vec}(\Phi) \text{diag}(\hat{\mathbf{g}}_k) \hat{\mathbf{H}}_r) (\mathbf{f}_k \mathbf{f}_k^H - \gamma_0 \sum_{i \neq k} (\mathbf{f}_i \mathbf{f}_i^H + \mathbf{F}_E \mathbf{F}_E^H)) \Delta^H \text{vec}(\Phi)^H \\ & + (\mathbf{h}_{d,k} + \text{vec}(\Phi) \text{diag}(\hat{\mathbf{g}}_k) \hat{\mathbf{H}}_r) (\mathbf{f}_k \mathbf{f}_k^H - \gamma_0 \sum_{i \neq k} (\mathbf{f}_i \mathbf{f}_i^H + \mathbf{F}_E \mathbf{F}_E^H)) \end{aligned}$$

$$\begin{aligned} & (\mathbf{h}_{d,k} + \text{vec}(\Phi) \text{diag}(\hat{\mathbf{g}}_k) \hat{\mathbf{H}}_r)^H - \gamma_0 \sigma^2 > 0, \\ \Leftrightarrow & \text{vec}(\Delta)^H \mathbf{A}_i \text{vec}(\Delta) + b_i^H \text{vec}(\Delta) + \text{vec}(\Delta)^H b_i + c_i > 0, \end{aligned}$$

where we have

$$\begin{aligned} \mathbf{A}_k &= (\mathbf{f}_k \mathbf{f}_k^H - \gamma_0 \sum_{i \neq k} (\mathbf{f}_i \mathbf{f}_i^H + \mathbf{F}_E \mathbf{F}_E^H)) \otimes (\text{vec}(\Psi) \text{vec}(\Psi)^H), \\ b &= \text{vec}(\text{vec}(\Phi) (\mathbf{h}_{d,k} + \text{vec}(\Phi) \text{diag}(\hat{\mathbf{g}}_k) \hat{\mathbf{H}}_r) (\mathbf{f}_k \mathbf{f}_k^H - \gamma_0 \sum_{i \neq k} (\mathbf{f}_i \mathbf{f}_i^H + \mathbf{F}_E \mathbf{F}_E^H))^H), \\ c &= (\mathbf{h}_{d,k} + \text{vec}(\Phi) \text{diag}(\hat{\mathbf{g}}_k) \hat{\mathbf{H}}_r) (\mathbf{f}_k \mathbf{f}_k^H - \gamma_0 \sum_{i \neq k} (\mathbf{f}_i \mathbf{f}_i^H + \mathbf{F}_E \mathbf{F}_E^H)) (\mathbf{h}_{d,k} + \text{vec}(\Phi) \text{diag}(\hat{\mathbf{g}}_k) \hat{\mathbf{H}}_r)^H - \gamma_0 \sigma^2. \end{aligned}$$

Lemma 1 is proved.

APPENDIX B PROOF OF PROPOSITION 1

Note that numerators and denominators in Eq. (9a) have the quadratic term $(\mathbf{h}_{d,k} + \mathbf{g}_k \Phi \mathbf{H}_r)$, we can convert Eq. (9a) into standard quadratic constraints, which is expressed as

$$\begin{aligned} & (\mathbf{h}_{d,k}^H + \text{vec}(\Phi)^H \text{diag}(\mathbf{g}_k^H) \mathbf{H}_r) (\mathbf{f}_k \mathbf{f}_k^H - \gamma_0 \sum_{i \neq k} (\mathbf{f}_i \mathbf{f}_i^H + \mathbf{F}_E \mathbf{F}_E^H)) \times (\mathbf{h}_{d,k}^H + \text{vec}(\Phi)^H \text{diag}(\mathbf{g}_k^H) \mathbf{H}_r)^H - \gamma_0 \sigma^2 > 0 \end{aligned} \quad (35)$$

By letting $\mathbf{f}_k \mathbf{f}_k^H - \gamma_0 \sum_{i \neq k} (\mathbf{f}_i \mathbf{f}_i^H + \mathbf{F}_E \mathbf{F}_E^H) = \mathbf{Y} \mathbf{Y}^H$ and substituting it into Eq. (35), we have

$$\|(\mathbf{h}_{d,k}^H + \text{vec}(\Phi)^H \text{diag}(\mathbf{g}_k^H) \mathbf{H}_r) \mathbf{Y}\|_2 - \gamma_0 \sigma^2 > 0. \quad (36)$$

By considering the triangle inequality $\|\mathbf{x}\mathbf{x}^H\|_2 \geq 2\text{Re}(\mathbf{x}^{[n]}\mathbf{x}^H) - \|\mathbf{x}^{[n]}\mathbf{x}^{[n]H}\|_2$ where $\|x\| = \|x^{[n]}\|$, the lower bound of Eq. (9a) is expressed as

$$\begin{aligned} & \text{Re}((\mathbf{h}_{d,k}^H + \text{vec}(\Phi^n)^H \text{diag}(\mathbf{g}_k^H)\mathbf{H}_r)(\mathbf{f}_k\mathbf{f}_k^H - \gamma_0 \sum_{i \neq k} \mathbf{f}_i\mathbf{f}_i^H) \\ & (\mathbf{h}_{d,k}^H + \text{vec}(\Phi)^H \text{diag}(\mathbf{g}_k^H)\mathbf{H}_r)^H - \|(\mathbf{h}_{d,k}^H + \text{vec}(\Phi^n) \\ & \times \text{diag}(\mathbf{g}_k^H)\mathbf{H}_r)\mathbf{Y}\|_2 - \gamma_0\sigma^2 > 0. \end{aligned} \quad (37)$$

By substituting $\text{diag}(\mathbf{g}_k^H)\mathbf{H}_r = \text{diag}(\hat{\mathbf{g}}_k^H)\hat{\mathbf{H}}_r + \Delta_k$ into Eq. (37), we can finally obtain Eq. (21).

APPENDIX C PROOF OF PROPOSITION 2

With fixed transmit covariance matrices $\{\mathbf{S}_1, \dots, \mathbf{S}_K, \mathbf{S}_E\}$, the optimal solution Φ^* satisfies that $E^{RF*} > E_0^{RF}$. Define the l -th auxiliary function for EU_l , which is expressed as

$$\begin{aligned} F_l(q_l) = & \sum_{i=l}^K ((\mathbf{h}_{d,i}^H + \mathbf{g}_i^H \Phi \mathbf{H}_r) \mathbf{S}_i (\mathbf{h}_{d,i}^H + \mathbf{g}_i^H \Phi \mathbf{H}_r)^H \\ & + (\mathbf{h}_{d,l}^H + \mathbf{g}_l^H \Phi \mathbf{H}_r) q_l \mathbf{S}_E (\mathbf{h}_{d,l}^H + \mathbf{g}_l^H \Phi \mathbf{H}_r)^H), \end{aligned} \quad (38)$$

where $0 \leq q_l \leq 1$. Therefore, we have $F_l(1) = E^{RF*} > E_0^{RF}$. If $F_l(0) < E_0^{RF}$, there exists a q_l satisfying $F_l(q_l) = E_0^{RF}$ since $F(q)$ is a continuous and monotonously increasing function. If $F_l(0) \geq E_0^{RF}$, we define $q_l = 0$. In this way, we have a sequence of $\{q_{K+1}, q_{K+2}, \dots, q_{K+L}\}$. Denote $q^* = \min\{q_{K+1}, q_{K+2}, \dots, q_{K+L}\}$. As a result, we have $F_l(q^*) \geq E_0^{RF}, \forall l$. Define a feasible solution, which is expressed as

$$\begin{cases} \mathbf{S}'_k = \mathbf{S}_1, & k = 1, 2, \dots, K \\ \mathbf{S}'_E = q^* \mathbf{S}_E, \\ \Phi' = \Phi^* \end{cases} \quad (39)$$

This solution satisfies the WET requirements, since we have $F_l(q^*) \geq E_0^{RF}, \forall l$. Then we consider the WDT performance. As for the DUs, the SINR of the k -th DU is expressed as

$$\begin{aligned} \gamma_k &= \frac{(\mathbf{h}_{d,k}^H + \mathbf{g}_k^H \Phi \mathbf{H}_r) \mathbf{S}_k (\mathbf{h}_{d,k}^H + \mathbf{g}_k^H \Phi \mathbf{H}_r)^H}{F_l(q_l^*) + \sigma^2} \\ &\geq \frac{(\mathbf{h}_{d,k}^H + \mathbf{g}_k^H \Phi \mathbf{H}_r) \mathbf{S}_k (\mathbf{h}_{d,k}^H + \mathbf{g}_k^H \Phi \mathbf{H}_r)^H}{F_l(1) + \sigma^2} \\ &\geq \gamma_0. \end{aligned} \quad (40)$$

Since $q^* \leq 1$, the power carried by the energy beams reduce. This results in the interference of the k -th DU reduces. Therefore, this new solution still satisfies the WDT requirements. Furthermore, we have $\text{Trace}(\sum_{i=1}^K \mathbf{S}'_i + \mathbf{S}'_E) \leq \text{Trace}(\sum_{i=1}^K \mathbf{S}_i + \mathbf{S}_E)$, due to reduced energy consumption for forming the energy beams. The proof is completed.

APPENDIX D PROOF OF PROPOSITION 3

The transmit covariance matrices are obtained from (P2.1) by using Kronecker product, which is difficult to analyse the performance of transmit covariance matrices. Therefore, we have to reformulated (P2.1). Since $\text{vec}(\Phi)$ is given, let $\mathbf{a} = \text{vec}(\Phi)^H \Delta$ satisfying $\|\mathbf{a}\| \leq$

$\delta \|\text{vec}(\Phi)\|$, $\mathbf{d}_k = (\mathbf{h}_{d,k}^H + \text{vec}(\Phi)^H \text{diag}(\hat{\mathbf{g}}_k^H)\hat{\mathbf{H}}_r)$ and $e_k = (\mathbf{h}_{d,k}^H + \text{vec}(\Phi)^H \text{diag}(\hat{\mathbf{g}}_k^H)\hat{\mathbf{H}}_r)(\mathbf{f}_k\mathbf{f}_k^H - \gamma_0 \sum_{i \neq k} (\mathbf{f}_i\mathbf{f}_i^H + \mathbf{F}_E \mathbf{F}_E^H))(\mathbf{h}_{d,k}^H + \text{vec}(\Phi)^H \text{diag}(\hat{\mathbf{g}}_k^H)\hat{\mathbf{H}}_r)^H - \gamma_0\sigma^2$. The SINR constraint of DU_k is reformulated as

$$\begin{aligned} & \mathbf{a}(\mathbf{S}_k - \gamma_0(\sum_{i \neq k} \mathbf{S}_i + \mathbf{S}_E))\mathbf{a}^H + \mathbf{a}(\mathbf{S}_k - \gamma_0(\sum_{i \neq k} \mathbf{S}_i + \mathbf{S}_E))\mathbf{d}_k^H \\ & + \mathbf{a}^H(\mathbf{S}_k - \gamma_0(\sum_{i \neq k} \mathbf{S}_i + \mathbf{S}_E))\mathbf{d}_k + e \geq 0. \end{aligned} \quad (41)$$

The energy constraints are converted in a similar way. Therefore, (P1.2) is equivalent to

$$(P1.3): \min_{\mathbf{S}_1, \dots, \mathbf{S}_K, \mathbf{S}_E} \text{Trace}(\sum_{i=1}^K \mathbf{S}_i + \mathbf{S}_E), \quad (42)$$

$$\text{s.t.} \begin{bmatrix} \mathbf{S}_k - \gamma_0 \mathbf{C}_i + \lambda \mathbf{I} & (\mathbf{S}_k - \gamma_0 \mathbf{C}_i)\mathbf{d}_k \\ \mathbf{d}_k^H (\mathbf{S}_k - \gamma_0 \mathbf{C}_i & e_k - \lambda \epsilon \end{bmatrix} \succeq 0, \quad k = 1, \dots, K, \quad (42a)$$

$$\mathbf{C}_i = \sum_{i \neq k} \mathbf{S}_i + \mathbf{S}_E, \quad k = 1, \dots, K, \quad (42b)$$

$$\begin{bmatrix} \sum_{i=1}^K \mathbf{S}_i + \mathbf{S}_E + \lambda \mathbf{I} & (\sum_{i=1}^K \mathbf{S}_i + \mathbf{S}_E)^H \mathbf{d}_l \\ \mathbf{d}_l^H (\sum_{i=1}^K \mathbf{S}_i + \mathbf{S}_E)^H & e_l - \lambda \epsilon \end{bmatrix} \succeq 0, \quad (42c)$$

$$l = K + 1, K + 2, \dots, K + L, \quad (42d)$$

$$\mathbf{S}_i \succeq 0 \quad i = 1, 2, \dots, K, \quad (42e)$$

$$\mathbf{S}_E \succeq 0, \quad (42f)$$

$$\lambda_i \geq 0 \quad i = 1, 2, \dots, K + L. \quad (42g)$$

Since (P1.3) is convex, the Lagrangian function of (P1.3) is expressed as

$$\begin{aligned} \mathcal{L} = & \delta \text{Trace}(\sum_{i=1}^K \mathbf{S}_i + \mathbf{S}_E) + \sum_{i=1}^K \mathbf{E}_i \mathbf{S}_i + \mathbf{E}_E \mathbf{S}_E \\ & + \sum_{k=1}^K \text{Trace}(\mathbf{P}_k \Upsilon_k(\mathbf{S}_1, \dots, \mathbf{S}_K, \mathbf{S}_E)) \\ & + \sum_{l=K+1}^{K+L} \text{Trace}(\mathbf{R}_l \Omega_l(\mathbf{S}_1, \dots, \mathbf{S}_K, \mathbf{S}_E)), \end{aligned} \quad (43)$$

where we have

$$\Upsilon_k(\mathbf{S}_1, \dots, \mathbf{S}_K, \mathbf{S}_E) = \mathbf{W}_k + \bar{\mathbf{H}}_k(\mathbf{S}_k - \gamma_0 \mathbf{C}_i)\bar{\mathbf{H}}_k^H, \quad (44)$$

$$\Omega_l(\mathbf{S}_1, \dots, \mathbf{S}_K, \mathbf{S}_E) = \mathbf{W}_l + \bar{\mathbf{G}}_l(\sum_{i=1}^K \mathbf{S}_i)\bar{\mathbf{G}}_l^H,$$

$$\mathbf{W}_k = \begin{bmatrix} \lambda_k \mathbf{I} & 0 \\ 0 & c_k - \lambda_k \epsilon \end{bmatrix}, \quad \mathbf{W}_l = \begin{bmatrix} \lambda_l \mathbf{I} & 0 \\ 0 & c_l - \lambda_l \epsilon \end{bmatrix},$$

$$\bar{\mathbf{H}}_k = [\mathbf{I}_N \quad \mathbf{d}_k], \quad \bar{\mathbf{G}}_l = [\mathbf{I}_N \quad \mathbf{d}_l].$$

The KKT conditions are then expressed as

$$\mathbf{E}_k - \delta \mathbf{I} + \bar{\mathbf{H}}_k \mathbf{P}_k \bar{\mathbf{H}}_k^H - \sum_{i \neq k} \bar{\mathbf{H}}_i \mathbf{P}_i \bar{\mathbf{H}}_i^H + \sum_l \bar{\mathbf{G}}_l \mathbf{R}_l \bar{\mathbf{G}}_l^H = 0, \quad (45)$$

$$\mathbf{E}_k \mathbf{S}_k = 0, \quad \mathbf{P}_k \Upsilon_k(\mathbf{S}_1, \dots, \mathbf{S}_K, \mathbf{S}_E) = 0,$$

$$\mathbf{R}_l \Omega_l(\mathbf{S}_1, \dots, \mathbf{S}_K, \mathbf{S}_E) = 0.$$

By multiplying the right-hand-side of Eq.(45) with \mathbf{S}_k , we have

$$(\delta\mathbf{I} - \bar{\mathbf{H}}_k \mathbf{P}_k \bar{\mathbf{H}}_k^H + \sum_{i \neq k} \bar{\mathbf{H}}_i \mathbf{P}_i \bar{\mathbf{H}}_i^H - \sum_{l=K+1}^{K+L} \bar{\mathbf{G}}_l \mathbf{R}_l \bar{\mathbf{G}}_l^H) \mathbf{S}_k = 0. \quad (46)$$

Denote that $\mathbf{X}_k = \delta\mathbf{I} - \bar{\mathbf{H}}_k \mathbf{P}_k \bar{\mathbf{H}}_k^H + \sum_{i \neq k} \bar{\mathbf{H}}_i \mathbf{P}_i \bar{\mathbf{H}}_i^H - \sum_{l=K+1}^{K+L} \bar{\mathbf{G}}_l \mathbf{R}_l \bar{\mathbf{G}}_l^H$ and $\mathbf{Y}_k = \delta\mathbf{I} + \sum_{i \neq k} \bar{\mathbf{H}}_i \mathbf{P}_i \bar{\mathbf{H}}_i^H - \sum_l \bar{\mathbf{G}}_l \mathbf{R}_l \bar{\mathbf{G}}_l^H + \mathbf{P}_k(1 : N_t, 1 : N_t)$. We have $\mathbf{X}_k = \mathbf{Y}_k - \mathbf{P}_k(N_t + 1, N_t + 1) \mathbf{d}_k \mathbf{d}_k^H$. Then we discuss about $\text{rank}(\mathbf{Y}_k)$. When \mathbf{Y}_k is full-rank, it results in $\text{rank}(\mathbf{X}_k) \geq N_t - 1$. Therefore, we have $\text{rank}(\mathbf{S}_k) = 1$. The optimal solution \mathbf{S}_k is expressed as $\mathbf{S}_k = a_0 \boldsymbol{\mu}_{k,0} \boldsymbol{\mu}_{k,0}^H$, where $\boldsymbol{\mu}_{k,0}$ spans the null space of \mathbf{X}_k . If $\text{rank}(\mathbf{Y}_k) = t < N_t$, denote $\mathbf{\Pi}_k \in \mathbb{C}^{N_t \times N_t - t}$ with $\mathbf{\Pi}_k (\mathbf{\Pi}_k)^H = \mathbf{I}$ as the orthogonal basis of the null space of \mathbf{Y}_k . Let $\boldsymbol{\mu}_{k,n} \in \mathbb{C}^{N_t \times 1}$ be the n -th column of $\mathbf{\Pi}_k$. According to [42], [43], we have $\mathbf{d}_k \mathbf{d}_k^H \mathbf{\Pi} = 0$. Therefore, the optimal solution \mathbf{S}_k is expressed as

$$\mathbf{S}_k = \sum_{n=1}^{N_t-t} a_n \boldsymbol{\mu}_{k,n} \boldsymbol{\mu}_{k,n}^H + a_0 \boldsymbol{\mu}_{k,0} \boldsymbol{\mu}_{k,0}^H. \quad (47)$$

We can then obtain a range of solutions $\{\mathbf{S}_1, \dots, \mathbf{S}_K, \mathbf{S}_E\}$. If $\text{rank}(\mathbf{S}_k) = 1$, we have $\bar{\mathbf{S}}_k = \mathbf{S}_k$. If $\text{rank}(\mathbf{S}_k) > 1$ for $\forall k = 1, \dots, K$, then we can obtain a new solution as

$$\bar{\mathbf{S}}_k = a_0 \boldsymbol{\mu}_{k,0} \boldsymbol{\mu}_{k,0}^H \quad (48)$$

$$\bar{\mathbf{S}}_E = \mathbf{S}_E + \sum_{n=1}^{N_t-t} a_n \boldsymbol{\mu}_{k,n} \boldsymbol{\mu}_{k,n}^H. \quad (49)$$

We can traverse this process from 1 to K . Then $\{\bar{\mathbf{S}}_1, \dots, \bar{\mathbf{S}}_K, \bar{\mathbf{S}}_E\}$ with $\text{rank}(\bar{\mathbf{S}}_k) = 1$ for $\forall k = 1, \dots, K$ can achieve the same performance as $\{\mathbf{S}_1, \dots, \mathbf{S}_K, \mathbf{S}_E\}$.

APPENDIX E CONVERGENCE ANALYSIS

The objective function of (P1.1) is continuous and the constraints are also continuous, while the constraints are continuous within a closed interval. Therefore, the optimum has an upper-bound. Let an auxiliary function $P_t(\mathbf{S}_1^{[n-1]}, \dots, \mathbf{S}_K^{[n-1]}, \mathbf{S}_E^{[n-1]}, \boldsymbol{\Phi}^{[n-1]})$ represent the transmit power, where $\{\mathbf{S}_1^{[n-1]}, \dots, \mathbf{S}_K^{[n-1]}, \mathbf{S}_E^{[n-1]}, \boldsymbol{\Phi}^{[n-1]}\}$ are the transmit covariance matrices and passive reflecting beamformer, respectively. During the $(n-1)$ -th iteration, the input to (P2.1) is $\boldsymbol{\Phi}^{[n-2]}$, which yields the objective value of $P_t(\mathbf{S}_1^{[n-1]}, \dots, \mathbf{S}_K^{[n-1]}, \mathbf{S}_E^{[n-1]}, \boldsymbol{\Phi}^{[n-2]})$. The output of (P2.1) is also the input to (P3.1). Then we obtained the solution to (P3.1) as $\boldsymbol{\Phi}^{[n-1]}$. Since the passive reflecting beamformer $\boldsymbol{\Phi}^{[n-1]}$ can improve both the WDT and WET performances, according to Proposition 2, the transmit power $P_t(\mathbf{S}_1^{[n]}, \dots, \mathbf{S}_K^{[n]}, \mathbf{S}_E^{[n]}, \boldsymbol{\Phi}^{[n-1]})$ reduces in the next iteration. Therefore, the objective value of (P1.1) monotonously decreases. The convergence of Algorithm 2 is proved.

REFERENCES

[1] P. Yadav and others., "Application of internet of things and big data towards a smart city," pp. 1–5, 2018.

[2] A. Anufrienko, "Appliances of smart tv as an iot device for industry 4.0," vol. 02, pp. 1–4, 2019.

[3] T. Taleb and others., "Machine type communications in 3gpp networks: potential, challenges, and solutions," *IEEE Communications Magazine*, vol. 50, no. 3, pp. 178–184, 2012.

[4] L. Chettri and others., "A comprehensive survey on internet of things (iot) toward 5g wireless systems," *IEEE Internet of Things Journal*, vol. 7, no. 1, pp. 16–32, 2020.

[5] J. Hu and others., "Energy self-sustainability in full-spectrum 6g," *IEEE Wireless Communications*, pp. 1–8, 2020.

[6] J. Hu and others., "Integrated data and energy communication network: A comprehensive survey," *IEEE Communications Surveys Tutorials*, vol. 20, no. 4, pp. 3169–3219, 2018.

[7] Z. Zhu and others., "Robust beamforming designs in secure mimo swipt iot networks with a non-linear channel model," *IEEE Internet of Things Journal*, pp. 1–1, 2020.

[8] D. Kudathanthirige and others., "Wireless information and power transfer in relay-assisted downlink massive mimo," *IEEE Transactions on Green Communications and Networking*, vol. 3, no. 3, pp. 789–805, 2019.

[9] A. S. d. Sena and others., "What role do intelligent reflecting surfaces play in multi-antenna non-orthogonal multiple access?," *IEEE Wireless Communications*, vol. 27, no. 5, pp. 24–31, 2020.

[10] J. Ye and others., "Joint reflecting and precoding designs for ser minimization in reconfigurable intelligent surfaces assisted mimo systems," *IEEE Transactions on Wireless Communications*, vol. 19, no. 8, pp. 5561–5574, 2020.

[11] S.-M. Park and others., "Joint antenna and device scheduling in full-duplex mimo wireless powered communication networks," *IEEE Internet of Things Journal*, pp. 1–1, 2022.

[12] C. Ma and others., "Massive mimo empowered wireless powered sensor networks: An optimal design with statistical csi," *IEEE Wireless Communications Letters*, pp. 1–1, 2022.

[13] Z. Zhu and others., "Secrecy rate optimization in nonlinear energy harvesting model-based mmwave iot systems with swipt," *IEEE Systems Journal*, pp. 1–11, 2022.

[14] J. Hu and others., "Multi-domain resource scheduling for full-duplex aided wireless powered communication network," *IEEE Transactions on Vehicular Technology*, pp. 1–13, 2022.

[15] Q. Wu and others., "Joint active and passive beamforming optimization for intelligent reflecting surface assisted swipt under qos constraints," *IEEE Journal on Selected Areas in Communications*, vol. 38, no. 8, pp. 1735–1748, 2020.

[16] Y. Zou and others., "Wireless powered intelligent reflecting surfaces for enhancing wireless communications," *IEEE Transactions on Vehicular Technology*, vol. 69, no. 10, pp. 12369–12373, 2020.

[17] C. Pan and others., "Intelligent Reflecting Surface Aided MIMO Broadcasting for Simultaneous Wireless Information and Power Transfer," *IEEE Journal on Selected Areas in Communications*, pp. 1–1, 2020.

[18] X. Shao and others., "Target sensing with intelligent reflecting surface: Architecture and performance," *IEEE Journal on Selected Areas in Communications*, vol. 40, no. 7, pp. 2070–2084, 2022.

[19] X. Hu and others., "Irs-based integrated location sensing and communication for mmwave simo systems," *IEEE Transactions on Wireless Communications*, pp. 1–1, 2022.

[20] Z. Yu and others., "Location sensing and beamforming design for irs-enabled multi-user isac systems," *IEEE Transactions on Signal Processing*, vol. 70, pp. 5178–5193, 2022.

[21] Z. Wang and others., "Channel estimation for intelligent reflecting surface assisted multiuser communications: Framework, algorithms, and analysis," *IEEE Transactions on Wireless Communications*, vol. 19, no. 10, pp. 6607–6620, 2020.

[22] Z. Zhou and others., "Joint transmit precoding and reconfigurable intelligent surface phase adjustment: A decomposition-aided channel estimation approach," *IEEE Transactions on Communications*, vol. 69, no. 2, pp. 1228–1243, 2021.

[23] G. T. de Araujo and others., "Channel estimation for intelligent reflecting surface assisted mimo systems: A tensor modeling approach," *IEEE Journal of Selected Topics in Signal Processing*, vol. 15, no. 3, pp. 789–802, 2021.

[24] G. Zhou and others., "Robust beamforming design for intelligent reflecting surface aided miso communication systems," *IEEE Wireless Communications Letters*, vol. 9, no. 10, pp. 1658–1662, 2020.

[25] H. Niu and others., "Robust design for intelligent reflecting surface assisted secrecy swipt network," *IEEE Trans. on Wire. Com.*, pp. 1–1, 2021.

- [26] Z. Zhang and others., "Robust and secure communications in intelligent reflecting surface assisted noma networks," *IEEE Communications Letters*, pp. 1–1, 2020.
- [27] W. Yan and others., "Passive beamforming and information transfer design for reconfigurable intelligent surfaces aided multiuser mimo systems," *IEEE Journal on Selected Areas in Communications*, vol. 38, no. 8, pp. 1793–1808, 2020.
- [28] G. Yu and others., "Design, analysis, and optimization of a large intelligent reflecting surface-aided b5g cellular internet of things," *IEEE Internet of Things Journal*, vol. 7, no. 9, pp. 8902–8916, 2020.
- [29] Y. Zheng and others., "Intelligent reflecting surface enhanced user cooperation in wireless powered communication networks," *IEEE Wireless Communications Letters*, vol. 9, no. 6, pp. 901–905, 2020.
- [30] S. Hong and others., "Robust transmission design for intelligent reflecting surface-aided secure communication systems with imperfect cascaded csi," *IEEE Transactions on Wireless Communications*, vol. 20, no. 4, pp. 2487–2501, 2021.
- [31] S. Zargari and others., "Robust active and passive beamformer design for irs-aided downlink miso ps-swipt with a nonlinear energy harvesting model," *IEEE Transactions on Green Communications and Networking*, vol. 5, no. 4, pp. 2027–2041, 2021.
- [32] K. Ntougias and others., "Probabilistically robust optimization of irs-aided swipt under coordinated spectrum underlay," *IEEE Transactions on Communications*, vol. 70, no. 4, pp. 2298–2312, 2022.
- [33] S. Hu and others., "Robust and secure sum-rate maximization for multiuser miso downlink systems with self-sustainable irs," *IEEE Transactions on Communications*, vol. 69, no. 10, pp. 7032–7049, 2021.
- [34] I.-M. Kim and others., "Wireless information and power transfer: Rate-energy tradeoff for equi-probable arbitrary-shaped discrete inputs," *IEEE Transactions on Wireless Communications*, vol. 15, no. 6, pp. 4393–4407, 2016.
- [35] S. Liu and others., "Deep denoising neural network assisted compressive channel estimation for mmwave intelligent reflecting surfaces," *IEEE Transactions on Vehicular Technology*, vol. 69, no. 8, pp. 9223–9228, 2020.
- [36] C. Y. and others., "Channel estimation and passive beamforming for intelligent reflecting surface: Discrete phase shift and progressive refinement," *IEEE Journal on Selected Areas in Communications*, vol. 38, no. 11, pp. 2604–2620, 2020.
- [37] E. Boshkovska and others., "Practical Non-Linear Energy Harvesting Model and Resource Allocation for SWIPT Systems," *IEEE Communications Letters*, vol. 19, no. 12, pp. 2082–2085, 2015.
- [38] S. Boyd and L. Vandenberghe, *Convex Optimization*. Convex Optimization, 2004.
- [39] G. Zhou and others., "A framework of robust transmission design for irs-aided miso communications with imperfect cascaded channels," *IEEE Transactions on Signal Processing*, vol. 68, pp. 5092–5106, 2020.
- [40] Y. Lu and others., "Global Energy Efficiency in Secure MISO SWIPT Systems With Non-Linear Power-Splitting EH Model," *IEEE Journal on Selected Areas in Communications*, vol. 37, no. 1, pp. 216–232, 2019.
- [41] Y. Hou and others., "Waveform shaping for wireless information and energy provision with carrier frequency offset," in *2021 IEEE International Conference on Communications Workshops (ICC Workshops)*, pp. 1–6, 2021.
- [42] L. Liu and others., "Secrecy wireless information and power transfer with miso beamforming," *IEEE Transactions on Signal Processing*, vol. 62, no. 7, pp. 1850–1863, 2014.
- [43] W. Wu and others., "Robust secure beamforming for wireless powered full-duplex systems with self-energy recycling," *IEEE Transactions on Vehicular Technology*, vol. 66, no. 11, pp. 10055–10069, 2017.

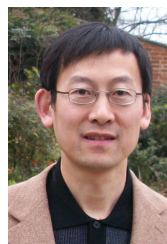


Qingdong Yue received his B.S degree from Chongqing University (CQU), China, in 2018. He is now studying for a Ph.D. degree at University of Electronic Science and Technology of China (UESTC). His research interests include simultaneous wireless information and power transfer, MIMO and intelligent reflecting surface.



Jie Hu [S'11, M'16, SM'21] (hujie@uestc.edu.cn) received his B.Eng. and M.Sc. degrees from Beijing University of Posts and Telecommunications, China, in 2008 and 2011, respectively, and received the Ph.D. degree from the School of Electronics and Computer Science, University of Southampton, U.K., in 2015. Since March 2016, he has been working with the School of Information and Communication Engineering, University of Electronic Science and Technology of China (UESTC). He is now a Research Professor and PhD supervisor.

He won UESTC's Academic Young Talent Award in 2019. Now he is supported by the "100 Talents" program of UESTC. He is an editor for *IEEE Wireless Communications Letters*, *IEEE/CIC China Communications and IET Smart Cities*. He serves for *IEEE Communications Magazine*, *Frontiers in Communications and Networks* as well as *ZTE communications* as a guest editor. He is a technical committee member of ZTE Technology. He is a program vice-chair for IEEE TrustCom 2020, a technical program committee (TPC) chair for IEEE UCET 2021 and a program vice-chair for UbiSec 2022. He also serves as a TPC member for several prestigious IEEE conferences, such as IEEE Globecom/ICC/WCSP and etc. He has won the best paper award of IEEE SustainCom 2020 and the best paper award of IEEE MMTC 2021. His current research focuses on wireless communications and resource management for B5G/6G, wireless information and power transfer as well as integrated communication, computing and sensing.



Kun Yang [M'00, SM'10, F'23] received his PhD from the Department of Electronic & Electrical Engineering of University College London (UCL), UK. He is a Chair Professor in the School of Computer Science & Electronic Engineering, University of Essex, leading the Network Convergence Laboratory (NCL), UK. He is also an affiliated professor at UESTC, China. Before joining in the University of Essex at 2003, he worked at UCL on several European Union (EU) research projects for several years. His main research interests include wireless

networks and communications, IoT networking, data and energy integrated networks and mobile computing. He manages research projects funded by various sources such as UK EPSRC, EU FP7/H2020 and industries. He has published 200+ journal papers and filed 20 patents. He serves on the editorial boards of both IEEE (e.g., IEEE TNSE, WCL, ComMag) and non-IEEE journals. He is an IEEE ComSoC Distinguished Lecturer (2020-2021) and a Member of Academia Europaea (MAE).



Kai-Kit Wong [M'01-SM'08-F'16] received the BEng, the MPhil, and the PhD degrees, all in Electrical and Electronic Engineering, from the Hong Kong University of Science and Technology, Hong Kong, in 1996, 1998, and 2001, respectively. After graduation, he took up academic and research positions at the University of Hong Kong, Lucent Technologies, Bell-Labs, Holmdel, the Smart Antennas Research Group of Stanford University, and the University of Hull, UK. He is Chair in Wireless Communications at the Department of Electronic

and Electrical Engineering, University College London, UK. His current research centers around 5G and beyond mobile communications. He is a co-recipient of the 2013 IEEE Signal Processing Letters Best Paper Award and the 2000 IEEE VTS Japan Chapter Award at the IEEE Vehicular Technology Conference in Japan in 2000, and a few other international best paper awards. He is Fellow of IEEE and IET and is also on the editorial board of several international journals. He is the Editor-in-Chief for IEEE Wireless Communications Letters since 2020.